Granite-Related Rare-Element Deposits and Experimental Constraints on Ta-Nb-W-Sn-Zr-Hf Mineralization

Robert L. Linnen[1] and Michel Cuney[2]

[1]Department of Earth Sciences, University of Waterloo, Waterloo, ON, N2L 3G1, rlinnen@uwaterlool.ca
[2]CNRS - CREGU, Université Henri Poincaré, BP 239, 54506 Vandoeuvre les Nancy, Cedex, France, cuney.michel@g2r.uhp-nancy.fr

Linnen, R.L., and Cuney, M., 2005, Granite-related rare-element deposits and experimental constraints on Ta-Nb-W-Sn-Zr-Hf mineralization, in Linnen, R.L., and Samson, I.M., eds., Rare-Element Geochemistry and Mineral Deposits: Geological Association of Canada, GAC Short Course Notes 17, p. 45-68.

INTRODUCTION

The "rare-elements" (also called rare-metals) are predominantly either large-ion-lithophile elements (LILE) or high-field-strength elements (HFSE), with low and high charge-to-ionic-radius ratios, respectively. Because of their sizes and/or charges, these elements do not readily substitute into most common rock-forming minerals, and thus behave incompatibly during the crystallization of metaluminous, peraluminous and peralkaline melts. They are concentrated in silicate melts by small degrees of partial melting or by high degrees of fractional crystallization. In the latter case, HFSE abundances in residual melts typically increase until saturation of a HFSE accessory phase such as zircon or monazite occurs. The processes by which LILE are concentrated are reviewed by London (this volume), and therefore will not be discussed. This chapter focuses on HFSE in Groups III-A, IV-A, V-A and VI-A on the periodic table, notably Y, REE, Sn, W, Zr, Hf, Nb and Ta. The abundances of Y and the REE are presented by Samson and Wood (this volume), and the concentrations of Sn, W, Zr, Hf, Nb and Ta in different mantle and crustal reservoirs are given in Table 1. It is clear that the latter group of elements is enriched in the crust, particularly in the upper continental crust (typically at the ppm or tens of ppm level, similar to Y and REE), relative to MORB or C-1 chondrite, where most of these elements are near the 1 ppm concentration level, or lower.

The major rare-element producing districts of the world are reviewed by Pollard (1995) and are dominantly associated with either peralkaline or peraluminous magmatism. Peralkaline-associated deposits include those associated with carbonatites, which are the world's primary source of Nb and REE (see Mitchell, this volume; Rankin, this volume), and Nb-REE-Y-Zr deposits that are related to peralkaline granites (see Salvi and Williams-Jones, this volume). Two families of the rare-element class of pegmatites are also recognised (Černý, 1991a). One family has a pattern of metal enrichment similar to peralkaline granites, being characterized by Nb>Ta, with high concentrations of Y, REE, Sc, Ti, Zr, Be, Th, U, and F). This family of pegmatite is named NYF (for the high Nb, Y and F contents, Černý, 1991a). Ercit (this volume) reviews REE mineralization in the NYF family of pegmatites as well REE enrichment in other types of pegmatites.

This chapter focuses on rare-element mineralization associated with granites and pegmatites, particularly those associated with peraluminous compositions. These pegmatites belong to the second family of rare-element pegmatites and they are particularly important because most of the world's Ta is produced from peraluminous pegmatites. This second family is enriched in Li, Cs and Ta and consequently is named 'LCT' pegmatites (Černý, 1991a). Among the present and past producers of Li and Ta, the most significant pegmatite deposits are Greenbushes (Ta, Li) and Wodgina (Ta) in Australia, Tanco (Ta, Li, Cs) in Canada, Bikita (Li) and Kamativi (Li, Sn) in Zimbabwe and Kenticha (Ta) in Ethiopia (see Fetherstone, 2004 for a summary of global Ta resources). Details on the Tanco pegmatite are discussed by Černý (this volume), and the LCT pegmatites in Ontario by Breaks et al. (this volume). Tantalum and lithium are also produced from peraluminous leucogranites that are chemically similar to LCT pegmatites at Yichun in China. Additional examples of granite-hosted mineralization are the Li-F-rich Beauvoir granite in France, a well-studied intrusion that contains sub-economic concentrations of Ta-Sn-W-Li-Be, and similar mineralization hosted by the granites at Orlovka, Russia. The evolution of rare-element peraluminous granites will be examined first because the distinction between magmatic and hydrothermal processes is more readily apparent for these rocks compared to pegmatites. The experimental constraints on the interpretation of the magmatic and hydrothermal enrichment of rare-elements in these granites and LCT pegmatites will then be examined.

Table 1. Abundances of different high field strength elements in different reservoirs

Element	Upper Continental Crust	Lower Continental Crust	N-MORB	C-1 Carbonaceous Chondrite
Sn	5.5	1.5	1.1	1.65
W	2.0	0.7	0.01	0.093
Nb	25	6	2.33	0.240
Ta	2.2	1.0	0.132	0.0136
Zr	190	70	74	3.82
Hf	5.8	2.1	2.05	0.103

Values for Upper Continental Crust and Lower Continental Crust are from Taylor and McLennan (1995), N-MORB from Sun and McDonough (1989), and C-1 Carbonaceous Chondrite from McDonough and Sun (1995).

RARE-ELEMENT GRANITES

Rare-element granites (also called rare-metal granites) generally represent the latest, most fractionated end members of a layered sequence in upwardly differentiated plutons (Kovalenko et al., 1970; Cuney et al., 1992; Yin et al., 1995). They are relatively quartz-poor and albite-rich, and host disseminated Ta-Nb mineralization, as well as Sn-W in stockworks that developed during a

magmatic-hydrothermal stage (e.g., Beauvoir; Cuney et al., 1992). The most complex succession of granitic facies is observed at the Khangilai massif, Transbaikalia, Russia (Syritso et al., 2001), where seven different granitic units are recognized (Figure 1). Rare-element granites are generally emplaced at shallow levels and may be subvolcanic, and miarolitic cavities are present in some intrusions. They occur as isolated bodies (Beauvoir, France; Cuney et al., 1992), as pegmatite swarms (La Chaise-Chédeville, France; Raimbault 1998), as rhyolitic (Richemont, France; Raimbault and Burnol, 1998) to microgranitic dykes (ongonites, Kovalenko and Kovalenko, 1976) or as volcanic rocks such as at Spor Mountain, Utah, which hosts the world's largest Be deposit (as bertrandite, $Be_4Si_2O_7(OH)_2$; Lindsey, 1977).

The upper contacts of rare-element granites are generally characterized by a particular facies called "stockscheider" (which in German means: separation between two granite stocks, or between the granite stock and country rock), in which a variety of structures can be developed. The most typical is the development of "plumose" feldspars rooted at the roof of the last granite injection and branching downward in a matrix of fine-grained granite. Mineral layering may also occur at the contact with enclosing rocks. Much of the research on rare-element granites before 1980 was conducted in the USSR and China. Since that time, an increasing number of studies have been undertaken in other parts of the world and more sophisticated approaches have been used: radiogenic and stable isotopes, in situ analysis of re-homogenized melt inclusions, experimental studies of melting and crystallization of granites in halogen-rich systems and metal solubility. One of the most comprehensive studies has been the investigation of the Beauvoir peraluminous rare-element granite, France. A 900 m continuously cored drill hole through this rare-element granite was systematically sampled and analysed (Cuney and Autran, 1987; Cuney et al., 1992; Raimbault et al., 1995).

Classification of Rare-Element Granites

Various classifications of the rare-element granites have been proposed, the most complex of these, with eight types, was proposed by Beus (1982). However, these can be regrouped into three major types of magmatic associations with highly specific geochemical and mineralogical characteristics (Kovalenko, 1978; Pollard, 1989a; Taylor 1992, Raimbault et al., 1991, 1995):

i) The peralkaline rare-element granites (ASI <1, where ASI refers to the alumina saturation index, i.e., the molar Al/[Na+K] ratio). These granites are characterized by very high abundances of F, REE, Y, Zr, Nb, high abundances of Th, Sn, Be, Rb, and U, high Nb/Ta, and low P contents (Table 2). The high Zr and Th contents are particularly useful for distinguishing peralkaline from other rare-element granites (Figure 2). Peralkaline granites are relatively rich in Fe and contain sodic amphiboles and/or pyroxene (aegirine, riebeckite, arfvedsonite). Lithium-F micas, zinnwaldite, polylithionite or astrophyllite, occur in limited amounts because Li enrichments are only moderate (100 to a few 1000 ppm). The rare-element granites of this association correspond to the riebeckite-albite gran-

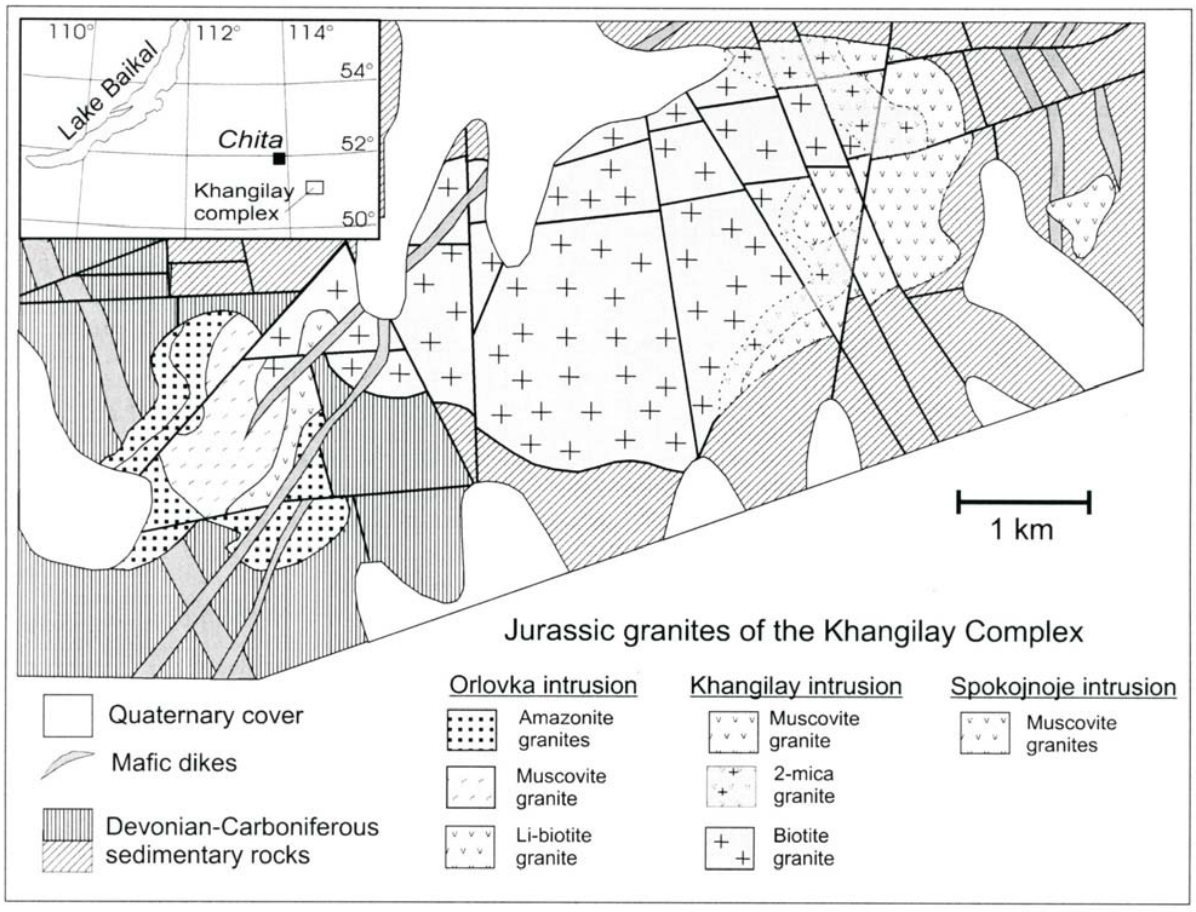

Figure 1. *Geology of the Khangily Complex, Russia, modified after Badanina et al., 2004.*

Table 2. Compositions of peralkaline granites

	1	2	3	4	5	6	7	8	9	10	11
n	6	1	2	3	6	7	11	1	1	1	1
SiO_2	76.6	74.9	76.1	76.5	71.6	67.18	67.9	68.8	69.94	71.25	72.39
TiO_2	0.74	0.38	0.14	0.14	0.23	0.77	0.51	0.36	0.27	0.33	0.34
Al_2O_3	8.96	10.4	10.88	11.09	13.54	5.62	9.66	10.29	12.38	11.26	9.18
Fe_2O_3	4.93	4.51	2.45	1.63	1.85			4.28	1.85	2.7	3.2
FeO			0.86	0.8	1.05	3.49	3.96	0.4	2.98	2.09	1.91
MnO	0.13	0.14	0.05	0.05	0.07	1.07	0.18	0.2	0.11	0.12	0.13
MgO	b.d.	b.d.	0.06	0.01	0.01	0	0.02	0.02	0.06	0.07	0.38
CaO	0.11	0.08	0.12	0.25	0.01	0.14	4.01	3.4	0.88	0.88	1.23
Na_2O	3.33	4.93	3.96	3.77	6.79	4.21	4.6	3.49	5.34	5.67	3.84
K_2O	5.19	4.67	4.56	4.97	3.79	4.73	3.69	4.79	4.84	3.95	4.03
P_2O_5		0.03	0.01	0.01	0.01	0.10	0.04	0.03	0.02	0.02	0.03
LOI	8.1	8.4	0.91	0.48	0.38			0.64	0.61	0.77	0.97
F(%)	0.94	1.22	0.1	0.22	0.94	1.99	0.87	1.97	0.58	0.61	0.48
ppm											
Cl						0.36	<0.05		198	203	128
B	0.19	0.48				12	68	14			
Li	210	126				230	721	119			
S	1624	1737	93	83	400						
As	24	55	12		0	320					
Ba			18	8	45	1400	164	176	70	67	58
Be						340	92	33			
Cs				1.4	0.7	8	1.4	1.4			
Ga						270			37	38	36
Hf			41	26	103	334	335				
Nb	1177	1946	434	245	1604	5750	991	1128	218	491	942
Pb			89	55	103		264	310			
Rb	1275	2042	396	411	1226	3770	390	666	469	752	1067
Sc				0.2	0.2		0.21	0.18			
Sn			50	17	50	660	277	470			
Sr	10	3.5	5	5	0	5	138	215	27	39	80
Ta				31	312		72	67			
Th	75	198	156	61	126	410	114	118	62	139	180
U						155	58	46	8	19	36
Y	425	304	234	590	144	2240	1042	1136	307	1328	1556
Zn			500	478	766		1347	1200	366	712	1198
Zr	3187	11494	1103	815	3071	26530	13920	17137	2465	6325	12429
La	92	109	28	139	70	520	629	750	271	246	1446
Ce	260	370	70	286	232	1450	1308	1448	570	531	1206
Pr	34	47				200	153	409	60	60	650
Nd	131	165				580	634	633	229	206	653
Sm	41	44				190	154	183	53	47	424
Eu	0.4					17	13.9	19	3	3	69
Gd	69	61					121	154	48	47	307
Tb	15	18				86	24.3	46	13	12	362
Dy	88	102				420	114	221	73	69	304
Ho	16	22				100	32	67	19	17	294
Er	41	84				290	72	160	66	46	269
Yb	52	148				49	113	138	62	51	375
Lu	8.4	22				42	19.4	14.4	9	8	367

1-2 – Melt inclusions of the peralkaline Amis complex, Namibia (Schmitt et al., 2000); 3-5 – Arfvedsonite albite granite, Nigeria (Kinnaird et al., 1985); 6 – Melt inclusion of the peralkaline Khaldzan-Buregtey complex, Mongolia (Kovalenko et al., 1995); 7-8 – Peralkaline granites of the Khaldzan-Buregtey complex, Mongolia, (7) 5th phase, (8) 7th phase (Kovalenko et al., 1995); 9-11 – Peralkaline granites of the Lac Brisson, Labrador, Canada (Pillet et al., 1992).

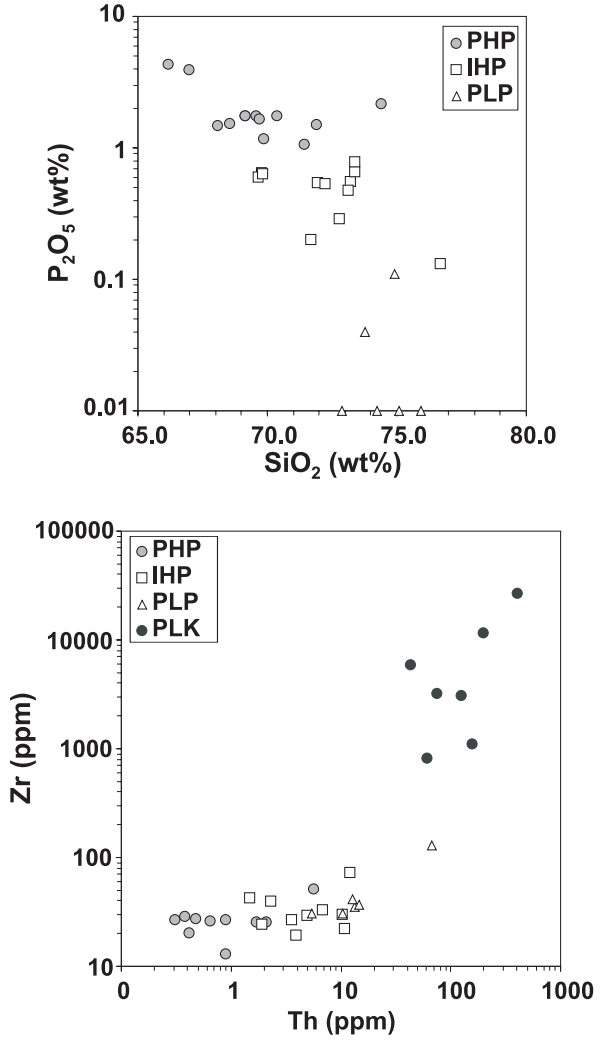

Figure 2. *Trace-element characteristics of peraluminous high phosphorous (PHP), peraluminous intermediate phosphorous (IHP), peraluminous low phosphorous (PLP) and peralkaline granites (PLK). See Tables 2 to 4 for the sources of data for the granites. Values for the Upper Continental Crust are from Taylor and McLennan (1995), except for fluorine, which is from Wedepohl (1995).*

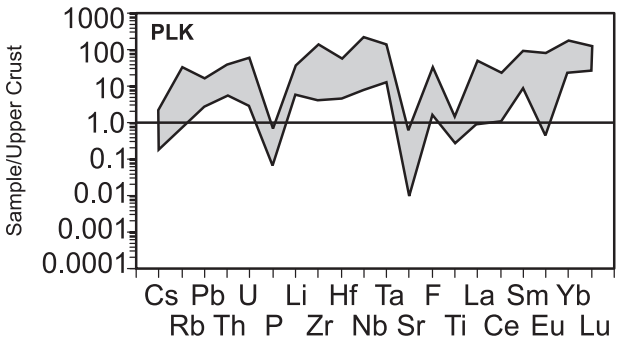

Figure 3. *Distribution of rare-elements in peralkaline granites (PLK) relative to the Upper Continental Crust. See Table 2 for the sources of data for the granites. Values for the Upper Continental Crust are from Taylor and McLennan (1995), except for fluorine, which is from Wedepohl (1995).*

ites of Beus et al. (1962), the agpaitic class of Kovalenko (1978), and belong to the highly fractionated A1-type granites of Eby (1992). Silica-undersaturated felsic peralkaline complexes are related to this type because they are characterized by the same type of metal enrichments. The peralkaline association is typically emplaced in anorogenic geotectonic settings. They generally contain Zr mineralization as zircon and zirconosilicates such as elpidite and gittingsite, Nb mineralization, mainly as pyrochlore, and REE mineralization, mainly as fluocarbonates rather than monazite. Figure 3 shows a spider diagram of concentrations of rare-elements in peralkaline granites relative to the upper crust. Of particular importance on this diagram are the high concentrations of the REE, and the relatively flat Zr-Hf-Nb-Ta profile.

ii) Metaluminous (molar $[Na_2O+K_2O]<Al_2O_3<[CaO+Na_2O+K_2O]$) to peraluminous (molar $Al_2O_3>[CaO+Na_2O+K_2O]$), low P (phosphorous) rare-element granites. These granites typically have intermediate REE, Y, Zr, Hf, Th, and Pb contents (Table 3). Their REE patterns are generally flat and with a strongly negative Eu anomaly (Figure 4). This type of rare-element granite is associated

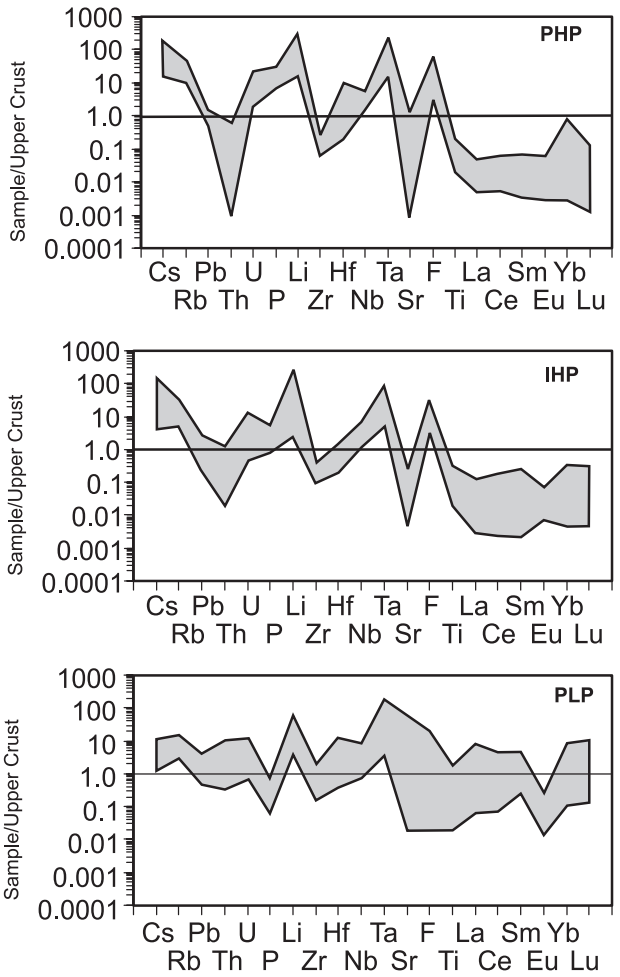

Figure 4. *Distribution of rare-elements in peraluminous high phosphorous (PHP), peraluminous intermediate phosphorous (IHP), peraluminous low phosphorous (PLP). See Tables 3 to 5 for the sources of data for the granites. Values for the Upper Continental Crust are from Taylor and McLennan (1995), except for fluorine, which is from Wedepohl (1995).*

Table 3. Compositions of peraluminous low phosphorous granites

	12	13	14	15	16	17	18	19	20	21	22	23	24
n	6	1	2	3	6	7	11	1	1	1	1	1	1
SiO_2	74.91	74.66	74.25	73.76	72.89	75.09	75.95	75.9	72.16	74.93	74.21	72.99	75.9
TiO_2	0.108	0.96	0.33	0.11	0.01	0.07	0.1	<0.01	0.01	0.02	0.01	0.01	0.11
Al_2O_3	14.55	13.34	14.01	14.99	16	13.61	12.9	13.44	15.92	13.73	14.67	15.1	12.85
Fe_2O_3	0.53	1.05	0.91	1.11	0.44	0.31	0.54	0.44	0.2	0.22	0.33	0.44	0.33
FeO						0.54	0.71						1.05
MnO	0.77	0.5	0.3	0.64	0.002	0.04	0.03	0.07	0.08	0.14	0.13	0.43	0.05
MgO	0.36	0.3	0.83	0.76	0.17	0.17	0.14	0.03	0.04	0.07	0.06	0.05	0.02
CaO	0.11	0.33	1.11	0.06	0.38	0.29	0.6	0.08	0.29	0.12	0.1	0.08	0.24
Na_2O	4.29	3.54	3.39	3.48	5.99	3.86	2.81	5.22	6.4	5.14	6.82	6.38	3.91
K_2O	3.65	4.46	4.76	5.1	3.27	4.62	5.34	3.89	3.73	4.04	1.81	2.72	4.31
P_2O_5	0.11	0	0.01	0.04	0.01	0.01	0.01	<0.01	<0.01	<0.01	<0.01	<0.01	0.01
LOI	1.09	1.56	1.37	1.19	0.81	0.86	1.25	0.73	0.74	1.31	0.64	1.19	0.52
F(%)	0.13	0.95		0.97	1.2	0.68	0.52						0.36
Li	76	544		605	1175	511	232	149		88			391
As	12.5		0.6	520		29	9						
Ba	30	12		25		49	59	33	26	52	16	23	109
Be	139				5	11	21						7
Bi						22	5	0.42	n.b.	2.94	n.b.	n.b.	
Cs	32		24	41	26	31.7	26.8	12	8	15	n.n.	5	
Ga	34		32	45	58			57	81	129	128	142	
Hf	2.5		2.8	2.3	8.9	5.6	6.6	30.01	28	23.76	38	75	28
Nb	88		19	39	52	74	48	44	50	71.51	33	52	214
Pb	29		29	9.5	39	22	28	69	83	65	36	29	56
Rb	1104	903	955	997	1229	1677	771	533	860	667	327	520	979
Sb	3.2		0.3	0.45	0.11	5	3	14.68	n.n.	0.9	n.n.	n.n.	
Sc	0.82		5.9	11.4	2.3			9.83	n.n.	4.78	2	3	
Sn	48	284	103	213	29	92	29	48	18	293	3888	1731	40
Sr	18.9	10	15	14.6	13.3	12	14	11	7	24	7	18	15
Ta	56		21	18	104	47.6	7.61	35	112	240.85	249	395	
Th	5.4		13.3	10.3	12.7	14.5	67.6	16.04	20	3.43	n.n.	12	111
U	2.7		12	6.9	2	29	31	5	n.n.	7	n.n.	7	
W	9.5	14	32	25	5	54	36	34	11	22	12	12	
Y	5.9	106	154	73	10.7	~6	102						696
Zn	44		10	62	108	45	27	275	92	138	657	302	376
Zr	30.3		35	30.3	41	37	130	155.9	49	44.26	47	75	399
	26	27	28	29	30	31	32	33	34	35	36	37	38
La	2	34.1	32	14.4	5.6	28	41						234
Ce	4.6	82	89	46.7	17.4	65	83						296
Nd	2.4	37.7	54	27	10								
Sm	1.15	12.4	21.4	10.6	2.6	6.33	9.92						
Eu	0.06	0.25	0.013	0.02	0.03	~0.005	0.13						
Tb	0.25	2.5	3.9	1.77	0.4	1.3	2.2						
Dy						2.29	5.09						
Ho						0.35	0.78						
Er						31	81						
Tm						0.021	0.004						
Yb	0.25	13.7	19.7	7.2	1.5	19	17.2						
Lu	0.044	1.85	3.49	1.31	0.23	2.16	2.23						
A/NK	1.32	1.25	1.31	1.33	1.20	1.20	1.24	1.05	1.09	1.07	1.11	1.12	1.16
Ta/Nb	0.64		1.11	0.46	2.00	0.64	0.16	0.80	2.24	3.37	7.55	7.6	

12 – Les Châtelliers granite, Vendée, France (Raimbault et al., 1995); 13 – Ahelehedj granite, Algeria (Cheilletz et al., 1992); 14 – Shizhuyuan topaz granite, Hunan, China (Raimbault et al., 1995); 15 – Chavance microgranite, Morvan, France (Raimbault et al., 1995); 16 – Orlovka albite-amazonite-cryophylite granite, Transbaikalia, Russia (Raimbault et al., 1995); 17-18 – Cinovec granite, Czech Republic (Breiter, 1998); (17) upper zinnwaldite-albite granite, (18) lower protolithionite granite; 19-23 – Nuweibi albite granite, Eastern Desert, Egypt (Renno, 1997); 24 – Biotite granite Ririwai complex, Nigeria (Kinnaird et al., 1985).

with high-K, calc-alkaline metaluminous rocks, rich in Th, REE, and Y (the higher Th and REE relative to high P granites are well illustrated by Figures 2 and 4). They correspond to the standard class of Kovalenko (1978), the highly fractionated I- or A2-type granites of Eby (1992), or the magnetite-series granites of Ishihara (1981). Zinnwaldite is the main, Fe-rich Li-F mica. Highly fractionated I and A2 types are difficult to distinguish because they tend to have similar geochemical characteristics (King et al., 1997, 2001). High K, calc-alkaline rare-element granites are significantly peraluminous, but less than the high P (phosphorous) type (see below) and are always associated with metaluminous to weakly peraluminous, less-fractionated intrusions. They occur in both post-orogenic and anorogenic geotectonic settings. The associated mineralization is mainly Nb-Ta-Sn as columbite-tantalite and cassiterite, and these granites have relatively low Zr/Hf and Nb/Ta ratios, as shown by the positive slope of the Zr-Hf-Nb-Ta profile on (Figure 4).

iii) The peraluminous (molar Al/[Na+K]>1.15) high P rare-element granites. These granites are characterized by extremely low REE (much lower than upper crust abundances, close to chondritic abundances; Figure 4), Y, Zr, Hf, Th, Sc, and Pb contents (Table 4), and by the presence of Li-rich muscovite or lepidolite (Li/F class of Kovalenko, 1978). Rubidium and Cs contents are also generally very high. Because of their strongly peraluminous character, they are classically related to the S-type granites of White and Chappell (1977). However, S-type granites have highly variable mineralogical and geochemical characteristics resulting from a variety of genetic processes (Stussi and Cuney 1993; Turpin et al., 1990). Peraluminous rare-element granites are generally associated with large, strongly peraluminous, muscovite-biotite leucogranitic plutons with a restricted variation of chemical composition. They were typically emplaced as post-orogenic plutons in continental collision belts such as the Variscan mid-European belt and the Jurassic (Yenshanian) belt of south-east China (e.g., Hu et al, 1984). Tantalum-Sn-Li mineralization in the form of microlite, columbite-tantalite, Ta-rich cassiterite, lepidolite, and amblygonite is associated with this type of granite. Figure 4 shows a very strong positive slope for the Zr-Hf-Nb-Ta profile of such granites, reflecting very low Zr/Hf and Nb/Ta ratios in these rocks, as well as very low Zr and Hf contents, and very high Ta abundances. It is also possible to distinguish a class of peraluminous granites with intermediate P contents (Figures 2 and 4; Table 5). Overall, the geochemical signature of the intermediate P granites is similar to the high P granites (Table 4).

The low and high P types of peraluminous rare-element granites represent the latest intrusions in the internal part of continental collision belts, and generally have been emplaced under extensional tectonic conditions. However, one occurrence, the Abu Rusheid albite-zinnwaldite rare-element granite in the Eastern Desert of Egypt was emplaced within a low angle thrust zone (M. Cuney, unpublished results). Such an exceptional, syntectonic emplacement is comparable to the tectonic setting of the giant Greenbushes rare-element pegmatite in Australia (Partington, 1990), as well as other LCT pegmatites (Breaks et al., this volume).

The peraluminous, high P rare-element granites are strongly enriched in F, variably enriched in Sn, W, Nb, Ta, Rb, Cs, Be and Li, and are depleted in Mg, Ti, and transition elements. Indium resources may also be associated with rare-element granites in indium-rich cassiterite or even indium minerals such as roquesite (CuInS; Botelho and Moura, 1998). Boron may be enriched (up to 4.1 wt.% B_2O_3 in melt inclusions, Thomas et al., 2003), but may be very low, even in highly F-, Li- and rare-element enriched bodies such as the Beauvoir granite (with only 20 ppm B, Cuney et al., 1992). Pollard et al. (1987) similarly divided Sn systems as being either F-rich or B-rich.

Origin of Peraluminous Rare-Element Granites

The main cause of rare-element enrichment in rare-element granites has been a controversial topic since the late 1950s, particularly among Russian geologists. The apical parts, or cupolas, of rare-element granites are commonly mineralized (e.g., with Nb, Ta, or Sn), and are also strongly enriched in volatiles (e.g., F, Li, P, and/or B). One group proposed a metasomatic origin for rare-element mineralization and another group favoured a magmatic origin. The "metasomatists" (Beus et al., 1962; Beus and Zhalashkova, 1964; Zhalashkova and Sitnin, 1967; Hu et al., 1984) proposed that the mineralized granites (apogranites) resulted from the upward movement of post-magmatic fluids that leached metals from the lower part of the pluton and concentrated them in the apical parts. It was argued that successive metasomatic zones of microclinization, albitization and greisenization could be recognized from the lower levels to the upper few hundreds meters of the pluton. By contrast, the "magmatists" (Kovalenko et al, 1970; Kovalenko and Kovalenko, 1976) maintained that the characteristics of the mineralized granites could have resulted entirely from crystal-melt fractionation, with only moderate redistribution during late- to post-magmatic fluid-rock interactions, which may have upgraded the mineralization. This model is based on the similarity of the whole rock compositions of rare-element granitoids and volcanic dykes (ongonites from Ongon, Mongolia; Kovalenko and Kovalenko, 1976), which indicates an essentially magmatic origin for at least some of the occurrences of rare-element mineralization. This model is also supported by more recent melt inclusion studies on peraluminous granites and pegmatites (e.g., Webster et al., 1997; Thomas and Webster, 2000; Badanina et al., 2004).

A well documented example of a rare-element peraluminous granite is the Beauvoir granite in France. The average major-element, trace-element, and oxygen isotopic compositions of this granite are similar to the Richemont rhyolite, which is a naturally quenched rare-element granite melt (compare Cuney et al, 1992 and Raimbault et al., 1995 with Raimbault and Burnol, 1998). Both of these are located in the northern Massif Central in France, and are likely related to the same magmatic event, which further strengthens a magmatic origin for rare-element enrichment in such granites. The unusual mineralogical and major-element compositions of rare-element granites can be explained by experimental studies of halogen-rich haplogranitic systems, which show that the granite minimum compositions shift toward albite-rich and quartz-poor granite compositions with increasing F and Li contents in the melt (Manning, 1981; Martin and Henderson, 1984). Finally, detailed studies of continuous drill core through rare-element granites have shown that upwardly differentiated layered sequences are the result of a series of magmatic injections (e.g., Gagny, 1987; Jacquot and Gagny, 1987; Cuney et al., 1992; Yin et al., 1995), with the most fractionated melt having been emplaced at the highest level. The thickness of the layered sequence is generally less than 300 m (Beus, 1982; Syritso and Chernick, 1967; Yin et al., 1995), but exceeds 700 m in the Beauvoir rare-element granite (Cuney et al., 1992).

In spite of the apparent magmatic origin for rare-element granites, it is still difficult to explain the extreme degree of element enrichments and depletions in such granites by common magmatic

Table 4. Compositions of peraluminous high phosphorous granites and melt inclusions

	25	26	27	28	29	30	31	32	33	34	35	36	37
n	11	15	13	6	15	23	6	32	2	1	1	1	1
SiO_2	67.0	66.2	68.54	69.15	68.09	69.17	69.57	71.46	71.9	69.88	70.37	74.41	69.7
TiO_2	0.04	0.1	0.01	0	0.01	0.01	0.01	0.01	0.01	0.01			0.02
Al_2O_3	15.5	15.9	17.58	16.74	17.35	17.22	16.86	16.1	15.88	16.47	17.07	14.42	16.44
Fe_2O_3			0.12	0.05	0.15	0.25	0.44	0.51	0.25	0.59	0.07	0.02	0.37
FeO	0.4	0.42									0.26	0.19	0.67
MnO	0.05	0.07	0.27	0.19	0.36	0.9	1.03	0.79	0.65	0.11	0.05	0.05	0.041
MgO	0.01	0.01	0.39	0.43	0.22	0.37	0.4	0.26	0.52	0.02			0.03
CaO	0.07	0.1	0.86	1.43	0.45	0.5	0.82	0.39	1.84	1.21	0.08	0.01	0.48
Na_2O	3.23	4.38	5.12	4.51	4.94	4.63	4.39	4.49	3.92	3.43	5.55	2.55	4.5
K_2O	4.45	4.27	3.46	2.78	3.33	3.37	3.56	3.67	2.35	3.12	2.37	2.75	3.51
P_2O_5	3.92	4.3	1.53	1.73	1.46	1.73	1.75	1.06	1.49	1.17	1.73	2.16	1.64
LOI	0.8	1.4	2.1	2.42	1.69	1.54	1.49	1.41	2.17	2.45	1.75	2.21	na
F(%)	3.84	3.46	1.77	1.71	2.51	2.22	1.67	1.66	0.19	1.25	0.47	0.53	1.48
ppm													
B	359	373	34	18	21	14	17	16	75	68	28	71	
Li	1590	319	5176	5057	5762	3738	2201	2296	1205	3072	2500	5532	1644
As			10.2	12.9	7.9	4	19	4.1	6.8	40.8			11
Ba			74	53	25	38	27	15	9	35.9	9	<5	
Be	221	139	283	286	97	34	11	27	3	92.1	83	385	
Bi	15	68											
Cs	689	341	676	546	360	378	204	255	136	362	60	350	111
Co			0.2	0.17	0.31	0.92	0.18	0.58	0.67				
Ga	76	56	64	60	51	38	33	32	36	34.4	29	52	
Hf	37	59	4	4.2	2.6	2.1	1.9	1.2	3.6	2.59	2.6	4.7	6.3
Mo	<1	<1	2.9	2.5	4	2.4	1.5	1.5		1.5			
Nb	103	117	130	116	91	49	39	49	95	85	67	46	124
Pb			26	25	29	16	11	10	18	18.1			<7
Rb	4900	4980	4265	3771	3440	2478	1768	2013	1473	1933	1140	2448	1812
Sb			0.617	0.672	0.541	0.153	0.249	0.115	0.29	2.05			
Sc			0.113	0.059	0.079	0.05	0.063	0.053	0.125				3.7
Sn	390	451	1099	1438	1175	961	590	347	1142	502	575	746	10
Sr	0.3	1.7	424	428	126	150	274	92	69	97.7	<5	<5	421
Ta	169	521	300	232	141	71	39	45	220	81.7	84	161	107
Th	6	6	2.1	1.7	0.65	0.48	0.38	0.42	0.9	0.31	0.01	0.9	5.7
U	45	64	13.8	13.5	11.3	15.9	18	14.9	6.4	14.2	5.4	15.4	31
W			70	55	44	35	22	30	19	54.6	17.5	5.9	76
Zn	19	52	65	54	80	119	144	127	112	91.0	69	58	84
Zr			25.5	25.6	25.7	27.4	28.3	20.2	26.3	26.8	12	13	51
La			0.64	0.36	0.76	0.73	0.77	0.65	0.79	1.37	0.248	0.145	0.9
Ce	<1	<1		0.61	1.78	1.24	1.46	1.01	0.87	2.66	0.434	0.337	4.1
Sm				0.047	0.072	0.068	0.073	0.054	0.063	0.309	0.044	0.015	0.12
Eu				0.009	0.011	0.008	0.005	0.007	0.018	0.055	0.0045	0.0025	0.057
Tb				0.007	0.013	0.009	0.007	0.004	0.014	0.074	0.0041	0.004	0.08
Yb	1.8	1		0.012	0.023	0.017	0.031	0.024	0.029	0.257	0.0261	0.0062	0.2
Lu				0.002	0.0032	0.0024	0.0041	0.0033	0.0048	0.041	0.0044	0.0004	0.035
A/NK	1.53	1.35	1.45	1.61	1.48	1.53	1.52	1.42	1.77	1.83	1.46	2.01	1.47
Ta/Nb	1.64	4.45	2.31	2.00	1.55	1.45	1.00	0.92	2.32	0.96	1.25	3.50	0.86

25-26 – Melt inclusions from the Ehrenfriedensdorf pegmatite, Germany (Webster et al., 1997); 27-32 – Beauvoir topaz lepidolite granite, Massif Central, France: fringe facies (27), upper B1 (28), B1 (29), B2 (30), B3 (31), B2 (32), (Raimbault et al., 1995); 33 – Montebras topaz muscovite granite, Massif Central, France (Raimbault et al., 1995); 34 – Richemont muscovite rhyolite, Massif Central, France (Raimbault et al., 1995); 35-36 – Argemela microgranite, Portugal; (35) microgranite, (36) differentaited ball facies (Charoy and Noronha, 1996); 37 – Podlesi granite, Czech Republic (Breiter, 1998).

Table 5. Compositions of peraluminous intermediate phosphorous granites and volcanic glass

	38	39	40	41	42	43	44	45	46	47	48	49
n	1	1	1	4	18	7	1	1	1	1	1	1
SiO_2	69.79	73.22	73.38	69.64	73.14	71.94	73.37	69.81	72.26	71.68	72.78	76.68
TiO_2	0.03	0.04	0.03	0.01	0.17	0.01	0.03	0.05	0.04	0.01	0.01	0.01
Al_2O_3	16.93	14.15	14.31	18.2	15.19	15.33	15.08	16.64	15.83	15.79	15.01	13.61
Fe_2O_3	0.16	0.11	0.41	0.05	1.37	0.72	0.41	1.1	0.04	0.01	0.09	0.13
FeO	0.6	0.91	na				na	na	0.57	0.84	0.58	0.46
MnO	0.052	0.037	0.042	1.12	0.63	0.48	0.04	0.03	0.06	0.09	0.16	0.06
MgO	0.02	0.03	0.01	0.02	0.33	0.66	0.04	0.09	0.02	0.24	0.12	0.12
CaO	0.24	0.47	0.54	0.12	0.54	0.51	0.58	0.46	0.22	0.60	0.34	0.52
Na_2O	5.19	3.8	5.54	6.14	3.75	4.08	5.01	2.83	4.14	5.84	5.34	4.86
K_2O	3.99	4.45	2.39	2.71	3.77	3.82	3.64	7.37	3.66	3.48	3.96	2.50
P_2O_5	0.645	0.55	0.65	0.59	0.47	0.54	0.78	0.63	0.53	0.20	0.29	0.13
LOI	Na	na	na	1.63	0.77	1.31	na	na	0.46	0.93	0.60	0.38
F(%)	1.45	1.07	0.2	1.84	0.8	0.53	0.381	0.427	1.33	0.37	0.44	0.86
ppm												
B				<20	<10				1958			
Li	901	975	51	5294	515	600	153	469	3200	166.8	98.8	77.7
As	16	17.4	0.2	0.9		3.1	4.6	26	13			
Ba					17	14			<10	7.6	38.8	16.3
Be				110					41.4			
Cs	125	130	16	482	31	71	60	121	566	90.7	54	39.3
Ga				39	34	32				62.2	34.3	35.7
Hf	2.46	2.23	1.2	3.7	1.8	1.8	1.48	1.88	<2	8	3.4	3.1
Nb	92	36	59	43	30	42	64	37	44	165.8	80.6	71.8
Pb	<7	<7	8		56	7	5	12	7	5.1	11.2	28.0
Rb	1515	1283	570	3423	883	1057	1244	1034	1177	1346	1412	861.3
Sc	2.6	4.1	0.32	0.025	2.1	4.4	0.19	9.5	2.2			
Sn	18	64	20	85	179	71	83	58	155	108.1	221.8	968.4
Sr	<7	16	87	4.2	69	56	33	21	1.62	17.7	17.4	14.0
Ta	55	15.3	33	186	11.1	20	30	12	26.9	130.1	122.6	146.4
Th	3.9	6.8	0.5	3.6	4.9	1.5	0.2	1.9	2.3	12.2	10.3	10.8
U	18	36	1.3	6.7	22.6	28.6	2.2	2.7	18.8	7.9	10.5	9.8
W	43	46	3.7	17	20	13	8.7	30		3.3	10.4	5.8
Zn	75	50	32	74	163	85	58	90	92	55.2	22.9	61.0
Zr	19	33	<7	26.4	29	42	<7	24	39	72.1	29.6	21.8
La	0.65	3.4	0.6	0.28	1	3.7	0.41	2.6	1.92	0.200	0.226	0.089
Ce	2.3	10.7	1.26	0.97	2.8	7.9	1	6.6	4.52	0.349	0.407	0.159
Pr										0.030	0.034	0.016
Nd				0.65	1.3	4.7				0.107	0.104	0.038
Sm		1.06	0.19	0.08	0.74	0.74	0.18	1.16	0.86	0.020	0.015	0.010
Eu	0.007	0.016	0.024	0.013	0.05	0.01	0.02	0.022	0.02	0.023	0.06	0.028
Gd									0.72	0.018	0.019	0.008
Tb	0.03	0.26	0.048	0.023	0.23	0.19	0.06	0.28		0.005	0.004	0.003
Dy									0.79	0.04	0.031	0.019
Ho										0.005	0.003	0.002
Er									0.35	0.012	0.011	0.008
Tm										0.002	0.002	0.002
Yb	0.12	0.7	0.13	0.01	0.25	0.37	0.11	0.61	0.39	0.065	0.036	0.038
Lu	0.018	0.1	0.016	0.0015	0.027	0.057	0.01	0.06	0.06	0.004	0.005	0.004
A/NK	1.32	1.28	1.22	1.40	1.48	1.41	1.24	1.32	1.47	1.18	1.15	1.27
Ta/Nb	0.60	0.43	0.56	4.33	0.37	0.48	0.47	0.32	0.61	0.78	1.52	2.04

38-39 – Podlesi granite, Czech Republic (Breiter, 1998); 40 – Sejby granite, Czech Republic (Breiter, 1998); 41 – Yichun topaz-lepidolite granite, Jiangxi, China (Raimbault et al., 1995); 42 – East Kemptville topaz-muscovite leucogranite, Nova Scotia, Canada (Kontak, 1990); 43-45 – Homolka muscovite granite, south Bohemian pluton, (43) (Raimbault et al., 1995), (44-45) (Breiter, 1998); 46 – Macusani volcanic glass pebble, Peru (Pichavant et al., 1987b); 47 – Shuiximiao topaz-albite granite, Limu district, China (Zhu et al., 2001); 48 – Laohutou topaz-albite granite, Limu district, China (Zhu et al., 2001); 49 – Jinzhuyuan topaz-albite granite, Limu district, China (Zhu et al., 2001).

processes. The high concentrations of fluxing elements such as F, Li, B, and P typical of rare-element granitic melts, are thought to have a key role in modifying melt structure and determining the physico-chemical properties of silicate melts (London, 1987), and the effects of these elements are thought to be additive (Dingwell, 1988; Linnen, 1998). They strongly decrease the viscosity and solidus temperature of the magmas, which facilitates crystal-melt separation and thus favours protracted crystal-melt fractionation, making it possible for extreme rare-element enrichment in the residual melts. The decrease of the Nb/Ta ratio with rare-element enrichment shows that mass-dependant fractionation processes, such as Soret diffusion (as proposed by Hildreth, 1979), cannot play an important role. The general location of the strongest rare-element enrichment at the roof of the pluton cannot be explained by in situ double diffusive convection involving sidewall crystallization. Where it has been possible to analyze complete transects of granite bodies, such as at the Beauvoir granite, other fractionation processes at the scale of each magmatic unit have been proposed. Raimbault et al. (1995) proposed that, in addition to crystal fractionation, liquid immiscibility may explain the extreme rare-element enrichment of the Beauvoir granite, with a brine/melt phase having transported elements such as Li, Rb, Ga, Sn, and Ta upward through the magma towards the roof of the granite body. In another example, Charoy and Noronha (1996) interpreted that the Argemela rare-element microgranite resulted from the injection of a quartz-albite-phengite crystal mush that was overprinted by a Li-F-P- and rare-element-rich phase. It is not clear whether the younger, rare-element-rich phase crystallized from a melt or a solution-melt derived from melt immiscibility at deeper levels. A similar process was proposed by Reyf et al. (2000) and Badanina et al. (2004) to explain the extreme rare-element enrichment in the Orlovka Ta deposit in the Khangilai complex, Russia. They proposed that the most Ta-rich part of the pluton resulted from the removal of an interstitial residual melt from deeper parts of the magmatic body that was injected into a previously solidified crystalline carapace at the top of the pluton. Gramenitskiy and Shchekina (2001) provided some experimental evidence for the partitioning of Nb, Ta, Zr and Hf into aluminofluoride melts coexisting with aluminosilicate melts. However, the aluminosilicate melts in these experiments were peralkaline, and it is not clear whether similar silicate-halide melt immiscibility will occur in peraluminous systems (see Veksler, this volume for further discussion). In order to further evaluate the various models of rare-element enrichment and crystallization of rare-element minerals in granitic systems, it is necessary to first examine the solubility and partitioning behaviour of the rare-elements in granitic systems.

EXPERIMENTAL CONSTRAINTS ON RARE-ELEMENT BEHAVIOUR

It is clear from the preceding sections that a magmatic model is currently favoured to explain rare-element mineralization. In order to assess this model, information on the mineral-melt partition coefficients of rare-elements are needed to constrain the degree of partial melting and the amount of fractional crystallization that are needed to produce the high degree of rare-element enrichment that is observed in rare-element granites and pegmatites. Knowledge of the solubilities of rare-element minerals in granitic melts is needed to assess the magmatic controls on rare-element mineralization and lastly, fluid-melt partition coefficients are required to assess the role of magmatic-hydrothermal fluids to mineralization. These data are reviewed below. It is also worth noting that there are a number of experimental studies that have investigated the behaviour of rare-elements in basaltic melts. However, the purpose of these studies is to better understand the mantle and the core, and the results are not directly applicable to granite-hosted ore deposits and thus will not be discussed. The partition coefficients, D, discussed below follow the normal definition where D_i^{a-b} represents the weight % of element i in phase a divided by weight % of element i in phase b.

Mineral-Melt Partitioning of Rare-Elements

The rare earth elements have long been used to understand petrogenesis in igneous systems and it is beyond the scope of this chapter to review all of the mineral-melt partition data for REE. The REE abundances of peraluminous granites and pegmatites are dominantly controlled by accessory phases, in particular monazite, xenotime, allanite, zircon, and apatite (e.g., Bea, 1996). The solubilities of these accessory phases in peraluminous melts are low, as discussed below, and consequently REE abundances in peraluminous granites are low, but their solubilities greatly increase with peralkalinity of the melts. Similarly, the Zr and Hf contents of peraluminous granites and pegmatites are low and are largely controlled by zircon-hafnon saturation and mineral-melt partition coefficients of Zr and Hf will not be considered further. By contrast, the abundances of Nb, Ta, W, and Sn are high in peraluminous rare-element granites and pegmatites, and as discussed above, these elements are believed to be enriched by fractional crystallization. Therefore this section discusses the mineral-melt partition coefficients of these elements.

Nb and Ta

Most of the mineral-melt partition data that have been determined either experimentally or from phenocrysts-matrix analyses are for basaltic systems. Linnen and Keppler (1997) showed that the relative solubilities of columbite-tantalite, and hence the relative magnitude of the Nb/Ta activity coefficient ratio in the melt, is strongly dependent on melt composition. Thus, partition coefficients for basalts cannot be applied to granites (similarly, partition coefficients for peralkaline granites cannot be applied to metaluminous or peraluminous granites). Nevertheless, some mineral-basalt melt partition data will be discussed here because of the paucity of partition data for granite melts. In basaltic systems Nb and Ta are modestly incompatible in ferromagnesian minerals. For pyroxenes, $D_{Nb}^{pyx-melt}$ and $D_{Ta}^{pyx-melt}$ varied as a function of $D_{Ti}^{pyx-melt}$ and the CaO content of the pyroxene (Forsythe et al., 1994), the ^{IV}Al content of the pyroxene (Hill et al., 2000), and the composition of the melt (Green et al., 2000). The only values for melts that are nearly granitic in composition are 0.065 for $D_{Nb}^{pyx-melt}$ and for 0.261 for $D_{Ta}^{pyx-melt}$, determined for clinopyroxene in a dacite melt at 1072°C and 0.1 MPa (Forsythe et al., 1994). Similarly, there are no amphibole-granite melt experimental partition coefficients, although Klein et al. (1997) determined partition coefficient values for a tonalite melt at 800 to 900°C and 1 GPa. At these conditions, $D_{Nb}^{amphibolite-melt}$ and $D_{Ta}^{amphibolite-melt}$ were both 0.3 to 0.4.

The minerals that are probably the most important in controlling Nb-Ta contents of igneous suites are the Fe-Ti oxide phases, most notably magnetite, titanite and ilmenite. Unfortunately, very few partition coefficients have been determined for such minerals in granitic melts. Linnen and Keppler (1997) calculated $D_{Nb}^{rutile-melt}$ and $D_{Ta}^{rutile-melt}$ values of ~4900 and ~1900, respectively, giving a D^{Nb}/D^{Ta} value of 2.6. These values are in contrast with the much lower values for more mafic melts, e.g., for an andesitic melt, Green and Pearson (1987) measured a $D_{Nb}^{rutile-melt}$ of 26.5 and $D_{Ta}^{rutile-melt}$ of 44.0 and a D^{Nb}/D^{Ta} value of 0.6. Horng and Hess (2000) determined

$D_{Nb}^{rutile–melt}$ and $D_{Ta}^{rutile–melt}$ values for granitic melts. However, the latter experiments were conducted for systems that were Fe- and Mn-free, and it is well established that Nb and Ta substitute into rutile via a columbite-type substitution (Černý and Ercit, 1985). Consequently Al^{3+} was involved to charge balance the 5+ substitution (i.e., $Al^{3+}+Nb^{5+}=2Ti^{4+}$), thus the partition values from Horng and Hess (2000) cannot be applied to natural rutile. Magnetite is also an important sink for Nb and Ta. For basaltic systems the partition coefficients for Nb and Ta ranged from <0.1 to ~3, depending on the magnetite composition (most notably they increased with increasing $D_{Ti}^{magnetite–melt}$; Nielsen and Beard, 2000). Ilmenite-andesite melt partition coefficients at 1000°C and 400 MPa determined by Green and Pearson (1987) were 4.6 and 6.6, for Nb and Ta, respectively, but much higher values are reported from analyses of a natural rhyolite: 51-71 and 64-85, respectively (Stimac and Hickmott, 1994). The only available partition data for titanite are from basaltic andesite, andesite and trachyte melt compositions at 950° to 1000°C and 400 to 750 MPa (Green and Pearson, 1987). Partition coefficients for titanite, $D_{Nb}^{tnt–melt}$ and $D_{Ta}^{tnt–melt}$, range from 3.5 to 7.6 and 10.6 to 19.6, respectively. It can be predicted that these values will be higher for granitic melts, similar to their partitioning behaviour with respect to rutile and ilmenite.

Some partition data was reported by Kovalenko et al. (1977) for naturally occurring ongonite (PLP) volcanic rocks, which are F- and rare-element-rich. Their results showed that quartz and feldspars contain negligible Nb and Ta. Partition coefficients derived for mica-groundmass pairs were 2.7 to 5.8 for $D_{Nb}^{mica–melt}$ and ~0.9 to 2.9 for $D_{Ta}^{mica–melt}$. The bulk distribution coefficients from that study showed the highly incompatible nature of Nb and Ta and ranged from 0.05 to 0.09 for Nb and 0.02 to 0.05 for Ta. More recently, Raimbault and Burnol (1998) determined partition coefficients for muscovite in the Li-F-P-rich (PHP) Richemont rhyolite dyke in France. $D_{Nb}^{mu–melt}$ is 3.5, whereas $D_{Ta}^{mu–melt}$ is 0.42, and Raimbault and Burnol (1998) proposed that muscovite crystallization could account for the decrease of Nb/Ta ratios observed in peraluminous granites.

Sn and W

We are not aware of any experimentally derived mineral-melt partition coefficients for Sn in granitic systems. However, it is very likely that in oxidized granitic melts Sn will be a compatible element because Sn^{4+} and Ti^{4+} have similar ionic radii and consequently melts will become depleted in Sn with magnetite and titanite crystallization. By contrast, in reduced melts Sn^{2+} behaves as an incompatible element (Lehmann, 1990). Partition coefficients for Sn have been derived from the analyses of phenocrysts and groundmass in sub-volcanic rocks (Kovalenko et al., 1977; Antipin et al., 1981; Kovalenko et al., 1988). Only magnetite and mica have partition coefficients >1. Raimbault and Burnol (1998) also reported a muscovite-rhyolite melt partition coefficient, but it was somewhat lower, at a value of 0.37.

There is also very little mineral-melt partition data for W and granitic melts. Candela and Bouton (1990) studied W partitioning in ilmenite at different oxygen fugacity (f_{O_2}) conditions. Values of $D_W^{ilm–melt}$ at 800°C and 100 MPa for a high-silica rhyolite melt ranged from 0.39 at the C-CH_4 buffer, to 0.5 at an f_{O_2} near the Ni-NiO buffer. Other partition coefficients are from natural rocks. In the studies of Kovalenko et al. (1977) and Antipin et al. (1981) mica was the only mineral that had a D value for W of >1. In the study of Kovalenko et al. (1988) D values near or above 1.0 were also reported for magnetite, K-feldspar and plagioclase at temperatures higher than 850°C.

Rare-Element Solubilities in Silicate Melts

Nb and Ta Mineral Solubilities

There is a wide variety of Nb-Ta minerals, and their compositions and structures have been reviewed by Foord (1982) and Černý and Ercit (1985). Only three groups of minerals are of significant economic importance: the pyrochlore, wodginite, and columbite-tantalite groups. Pyrochlore ($[A_{2-m}B_2O_6(O,OH,F)_{1-n}]$ where A=Ba, Bi, Ca, Ce, K, Na, Pb, Sn, Sr, Th, Sb^{3+}, U, Y, or Zr; and B=Nb, Ta, or Ti) is an important Nb mineral in carbonatites and other anorogenic intrusions (Černý and Ercit, 1989). The solubility of pyrochlore and other Nb phases in carbonatite melts is summarized by Mitchell (this volume). In peraluminous pegmatites, the pyrochlore-group mineral microlite $[(Ca,Na)_2Ta_2O_6(O,OH,F)]$ can be common, but typically is a subordinate Ta mineral, e.g., in the Tanco deposit (Černý et al. 1998). It is generally unclear whether it is a primary magmatic mineral or resulted from the replacement of previously crystallized Ta minerals. In the Greenbushes pegmatite, microlite is interpreted to be hydrothermal in origin (Partington et al., 1995), but by contrast, microlite is observed to be replaced by tantalite in the Beauvoir granite (Ohnenstetter and Piantone, 1992). Wodginite ($MnSnTa_2O_8$; for substitutions see Ercit et al., 1992) is an important ore mineral in the world's largest tantalum deposits, e.g., Tanco (Černý et al., 1998), Greenbushes (Partington et al., 1995), and Wodgina (Sweetapple and Collins, 2002), but the solubilities of microlite or wodginite in granitic melts have not yet been determined.

The columbite-tantalite $[(Fe,Mn)(Nb,Ta)_2O_6]$ group is the most abundant group of Nb-Ta minerals (Černý and Ercit, 1989) and the solubilities of manganocolumbite and manganotantalite in granitic melts have been the subject of several studies (Keppler, 1993; London, 1995; Horng and Hess, 1995; Linnen and Keppler, 1997; Linnen, 1998; Linnen, 2005). The Mn end-members were investigated because at geologically reasonable redox conditions Mn will have a 2+ valence in silicate melts (Linnen and Keppler, 1997); this is in contrast to the Fe end-members which require careful redox control (see below). Manganocolumbite and manganotantalite dissolve congruently in most granitic melt compositions:

$$Mn^{2+}Nb_2O_6^{crystal} = Mn^{2+}O^{melt} + Nb_2O_5^{melt} \quad (1)$$

and

$$Mn^{2+}Nb_2O_6^{crystal} = Mn^{2+}O^{melt} + Nb_2O_5^{melt} \quad (2)$$

Their solubilities are expressed as solubility products, K_{sp}^{Nb} and K_{sp}^{Ta}, defined as $[MnO]\cdot[Nb_2O_5]$, and $[MnO]\cdot[Ta_2O_5]$, respectively, where square brackets represent concentrations in mole/kg in the melt. The solubility products are related to the thermodynamic equilibrium constants of columbite (K^{Nb}) and tantalite (K^{Ta}) dissolution through the equations:

$$K^{Nb} = \gamma_{melt}^{Nb_2O_5} \cdot \gamma_{melt}^{MnO} \cdot X_{melt}^{Nb_2O_5} \cdot X_{melt}^{MnO} / a_{\text{mineral}}^{MnNb_2O_6} = \gamma_{Nb_2O_5} \cdot \gamma_{MnO} \cdot K_{sp}^{Nb} / a_{\text{mineral}}^{MnNb_2O_6} \quad (3)$$

$$K^{Ta} = \gamma_{melt}^{Ta_2O_5} \cdot \gamma_{melt}^{MnO} \cdot X_{melt}^{Ta_2O_5} \cdot X_{melt}^{MnO} / a_{\text{mineral}}^{MnTa_2O_6} = \gamma_{Ta_2O_5} \cdot \gamma_{MnO} \cdot K_{sp}^{Ta} / a_{\text{mineral}}^{MnTa_2O_6} \quad (4)$$

where γ represents the activity coefficients and X represents the

molar fractions in the melt phase, and *a* represents the activity of the crystalline phase. Depending on the choice of standard state, the activities of the minerals (pure phases) are unity. If one divides equation 3 by 4, the activity coefficient for MnO cancels out and one obtains the relationship:

$$K_{sp}^{Nb}/K_{sp}^{Ta} = (K^{Nb}/K^{Ta})\cdot(a_{mineral}^{MnNb_2O_6}/a_{mineral}^{MnTa_2O_6})\cdot(\gamma_{melt}^{Ta_2O_5}/\gamma_{melt}^{Nb_2O_5}) \quad (5)$$

The terms (K^{Nb}/K^{Ta}) and $(a_{mineral}^{MnNb_2O_6}/a_{mineral}^{MnTa_2O_6})$ are constant at fixed temperature and pressure. Thus, changes in the relative solubilities $(K_{sp}^{Nb}/K_{sp}^{Ta})$ with melt composition at constant temperature and pressure are inversely proportional to the relative activity coefficients of the metal oxide components in the melt $(\gamma_{melt}^{Ta_2O_5}/\gamma_{melt}^{Nb_2O_5})$. Linnen and Keppler (1997) showed that the solubility products of $MnNb_2O_6$ and $MnTa_2O_6$ are nearly identical in hydrous peralkaline granitic liquids at fixed P and T (Figure 5), but that the solubility product of $MnNb_2O_6$ is smaller than that of $MnTa_2O_6$ in water-saturated metaluminous and peraluminous melts. Columbite-tantalite evolution in most natural pegmatites is characterized by decreasing Nb/Ta (Figure 6). This is explained by the experimental data because manganocolumbite, being less soluble, will crystallize before manganotantalite, leading to Ta enrichment relative to Nb in the residual melt. The higher solubility of manganotantalite relative to that of manganocolumbite also explains the decrease in the Nb/Ta ratio with fractionation that typifies rare-element metaluminous and peraluminous granites and pegmatites (Figure 7). Because the activity coefficient of Ta in the melt is smaller than that of Nb, fractional crystallization will result in a progressive decrease of the Nb/Ta ratio, even if columbite-tantalite is not one of the phases that has crystallized. By contrast, because K_{sp}^{Nb} and K_{sp}^{Ta} are nearly identical in peralkaline granitic melts, fractional crystallization of this melt composition will not lead to a strong decrease of the Nb/Ta ratio with fractionation (Figure 7).

The solubilities of the Fe end-members (ferrocolumbite and tapiolite) are more complicated because they will depend on redox conditions:

$$Fe^{2+}Ta_2O_6^{crystal} = Fe^{2+}O^{melt} + Ta_2O_5^{melt} \quad (6)$$

but

$$Fe^{2+}O^{melt} + 0.5O_2^{melt} = Fe^{3+}O_{1.5}^{melt} \quad (7)$$

and combining reactions (7) and (8)

$$Fe^{2+}Ta_2O_6^{crystal} + 0.5O_2^{melt} = Fe^{3+}O_{1.5}^{melt} + Ta_2O_5^{melt} \quad (8)$$

It thus can be predicted from equation (8) that tapiolite solubility will increase with increasing f_{O_2}. Preliminary results of ferrocolumbite and tapiolite solubility in water-saturated haplogranitic melts (ASI=1.0) at 800°C, 200 MPa and at a log f_{O_2} of Ni-NiO+0.5 are 1.0×10^{-3} mol^2/kg^2 for ferrocolumbite and 2.3×10^{-3} mol^2/kg^2 for tapiolite (Linnen, unpublished data). These solubilities are an order of magnitude higher than those of the Mn end-members at the same conditions (1.2×10^{-4} mol^2/kg^2 and 2.6×10^{-4} mol^2/kg^2 for manganocolumbite and manganotantalite solubility, respectively; Linnen and Keppler, 1997). The higher solubilities of the Fe end-members mean that, if columbite-tantalite crystallization controls the Fe-Mn concentrations in granitic melts, an Fe-enrichment trend should be observed. This is opposite of the observed 'normal' magmatic trend of Mn enrichment in columbite-tantalite (Černý et al. 1986), indicating that one or more other phases controls Fe-Mn in rare-element granites and pegmatites. One possible explanation is that a silicate phase controls Fe-Mn contents. It is unlikely that this phase is garnet, because garnet is rarely present in rare-element granites and pegmatites, and a typical magmatic trend for this mineral is one of

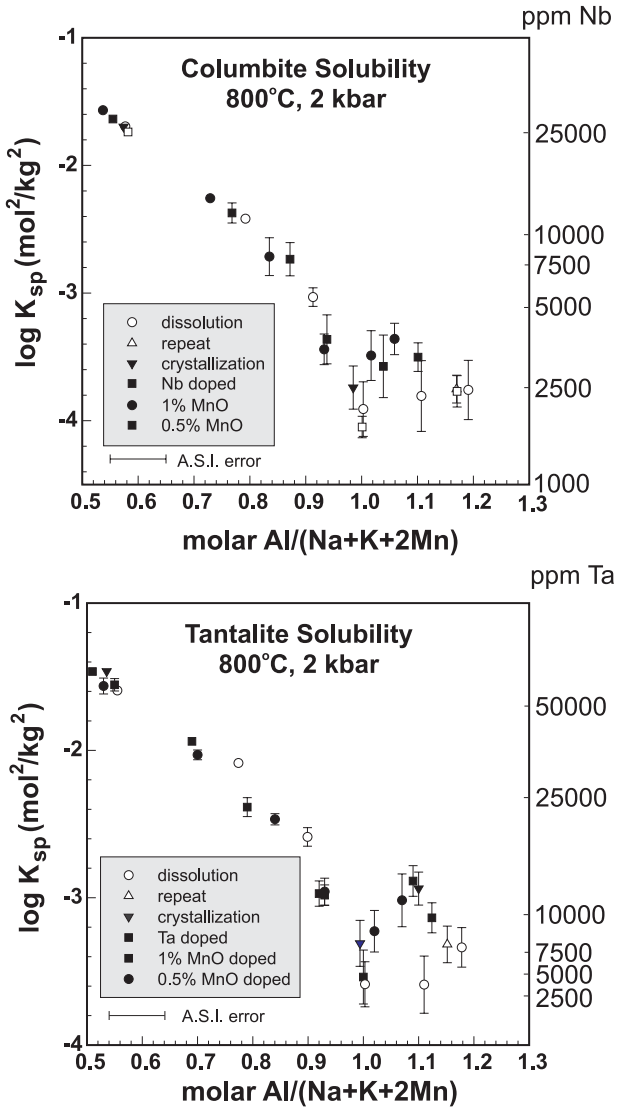

Figure 5. *Manganocolumbite-manganotantalite solubility in peralkaline to peraluminous haplogranitic melts at 800°C and 200 MPa. The ppm Nb and Ta scales are based on stoichiometry dissolution/saturation of $MnNb_2O_6$ and $MnTa_2O_6$, respectively. Modified after Linnen and Keppler (1997).*

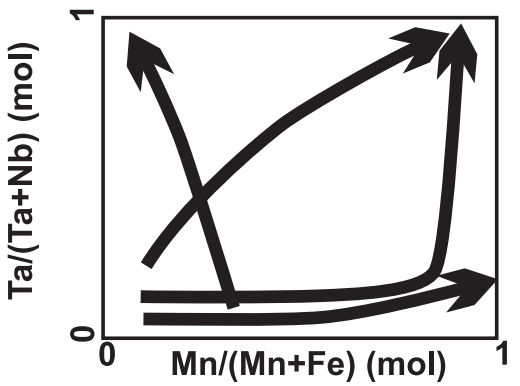

Figure 6. *Typical trends for columbite-tantalite compositions in LCT pegmatites. Modified after Černý et al. (1986).*

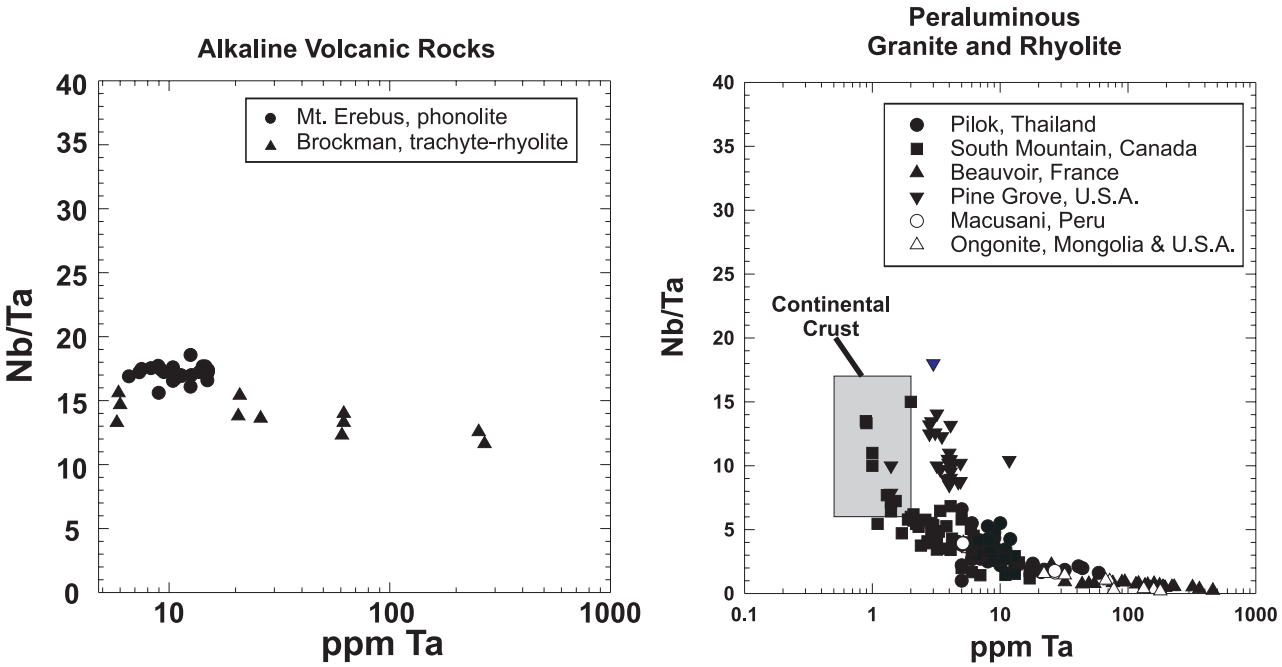

Figure 7. *Nb/Ta versus Ta in peralkaline and peraluminous granitic rocks. Symbols for the alkaline volcanic rocks are: solid circles, Mt. Erebus phonolite and solid triangles, Brockman trachyte-rhyolite. Symbols for the peraluminous granite and rhyolite are: solid circles Pilok granite, solid squares South Mountain granite, solid triangles, Beauvoir granite, solid inverted triangles Pine Grove granite, open circles Macusani rhyolite, and open triangles, Ongon rhyolite. Modified after Linnen and Keppler (1997).*

Fe-enrichment (Mn-rich cores and Fe-rich rims; e.g., Manning, 1983; Linnen and Williams-Jones, 1993; London et al., 2001). By contrast, tourmaline can show Mn-enrichment with fractionation (Selway et al. 2000; London et al., 2001), and thus the Mn enrichment observed in columbite-tantalite may be controlled by tourmaline crystallization. However, it should be noted that tourmaline is rare or absent in many rare-element pegmatites, e.g., in the Marko's pegmatite, Separation Lake area, Ontario, and columbite-tantalite at these pegmatites also display Mn-Ta enrichment (Tindle and Breaks, 2000). Thus, tourmaline crystallization cannot explain all of the Mn-enrichment trends observed in pegmatites.

Muscovite crystallization is potentially important in controlling Mn/Fe in the melt. Raimbault and Burnol (1998) reported muscovite-matrix partition values for the Richemont rhyolite dyke of 8.5 for $D_{Fe}^{mu-melt}$ and 2.0 for $D_{Mn}^{mu-melt}$, i.e., a $D_{Fe/Mn}^{mu-melt}$ value of 4.25, indicating that a melt will become strongly depleted in Fe relative to Mn with progressive muscovite crystallization. However, London et al. (2001) proposed that Mn substitution in tourmaline is coupled with Li and Al, thus Fe-Mn partitioning in micas may be a complex function of mica composition. A strong increase of the Mn/Fe ratio was observed for the **global evolution** of zinnwaldite-lepidolite, from the least to most fractionated Beauvoir granite (from 0.14 in the zinnwaldite-dominant composition at -865 m, to 0.28 in the lepidolite-dominant composition at -110 m; Monier et al., 1987). The same general evolution is observed in the Nb-Ta minerals, which represent negligible hosts for Fe and Mn compared to micas. However, **in detail**, the Mn/Fe ratios of zoned micas decrease from core to rim in a relatively fractionated phase of the Beauvoir granite (-429.25 m, Table 3 of Monier et al., 1987), which may correlate to Mn enrichment of the melt. An alternate explanation for the enrichment of Mn relative to Fe is that it is related to high F activities in the melt (Černý and Nemec, 1995), but experimental data is also needed to test this hypothesis.

The above experiments contain only H_2O as a fluxing compound, but it has been shown above that other fluxes such as F, Li, B and P, are important, and in fact characteristic of rare-element granites. The effects of these fluxes on the solubilities of manganocolumbite and manganotantalite in granitic melts have been the subject of several studies. Keppler (1993) demonstrated that the solubilities of manganocolumbite and manganotantalite both increase with increasing F contents of subaluminous (ASI=1.0) granitic melts. In that study it was shown that the solubilities of both manganocolumbite and manganotantalite increased approximately four- to five-fold as the F content of the melt increased from 0 to 6 wt.% F, thus there is no evidence that F should affect the Nb/Ta ratio of columbite-tantalite during crystal fractionation. The preliminary work of Wolf and London (1993) and Wolf et al. (1994) suggested that B has no effect on solubilities, but that P apparently increased their solubilities. Linnen (1998) showed that manganocolumbite and manganotantalite solubilities increase with increased Li content of the melt, and that the effects of F and Li were additive.

Most of the above solubility experiments were conducted at ≥800°C. These temperatures are high enough for the diffusion of Nb and Ta to be sufficiently fast for the melts to attain saturation in these phases over a reasonable experimental time scale (weeks to months), i.e., that the analyses of Fe, Mn, Nb, and Ta in quenched melts (glasses) reflect mineral saturation. In order to model the crystallization of columbite-tantalite in natural melts, the solubility data must be extrapolated to lower temperatures (Linnen and Keppler, 1997; Linnen, 1998). These data are summarized by Figure 8, where the ppm Nb or Ta represent stoichiometric ratios of Mn:Nb or Mn:Ta in the melt (i.e., ratios of 0.5) for saturation of manganocolumbite and manganotantalite. The amounts of Nb and Ta in the melt at saturation could be lower if the Mn contents were correspondingly higher, however, high Mn contents in peraluminous melts will result in spessartine crystallization, and for that rea-

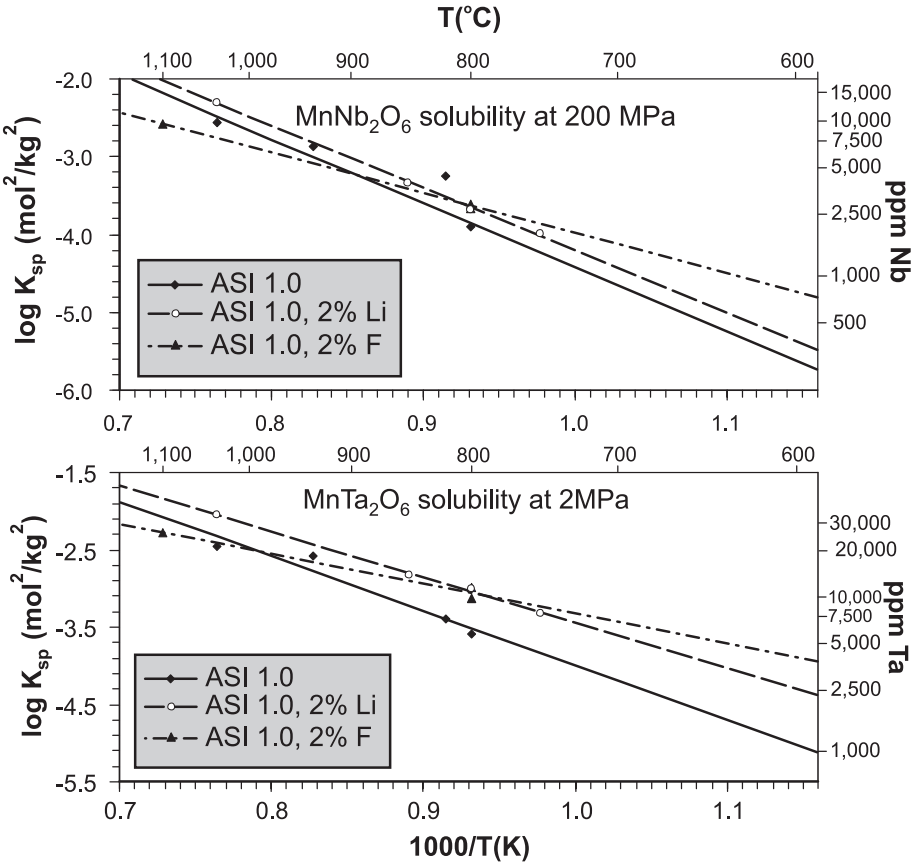

Figure 8. *Temperature dependence and the effects of Li and F on manganocolumbite-manganotantalite solubility in subaluminous haplogranitic melts at 200 MPa. The ppm Nb and Ta scales are based on stoichiometric dissolution/saturation of $MnNb_2O_6$ and $MnTa_2O_6$, respectively. The data is from Linnen (1998).*

son Linnen and Keppler (1997) and Linnen (1998) calculated the amount of Nb and Ta required for manganocolumbite-manganotantalite saturation in a melt with 0.05 wt.% Mn. At these conditions, 70, 120 and 120-490 ppm Nb are required for manganocolumbite saturation in melts with 0 wt.% Li-F, 2 wt. % Li, and 2 wt.% F, respectively, and 510, 2700 and 1300-6800 ppm Ta are required for manganotantalite saturation in water saturated melts at 600°C and 200 MPa with 0 wt.% Li-F, 2 wt. % Li, and 2 wt.% F, respectively.

Zr, Hf and REE Mineral Solubilities

Magmatic zirconium minerals in peralkaline silicate rocks include zirconosilicates such as eudialyte, elpidite and wadeite, in addition to zircon and baddeleyite. Discrete Hf minerals are not present in such rocks. A number of rare earth minerals are also present in peralkaline rocks, notably fluorcarbonate minerals such as bastnäsite (see Ewing and Chakoumakos, 1982, for a detailed list of Zr, Hf, and REE minerals). The solubilities and stabilities of these minerals are poorly understood, but Marr et al. (1998) established that in H_2O-saturated, peralkaline granitic-syenitic melts (ASI=0.73) at 800°C and 100 MPa, zircon was the stable Zr phase in melts with greater than ~55 wt.% SiO_2. At lower silica contents, either wadeite or baddeleyite was the stable Zr phase. Marr et al. (1998) also noted that a solubility maximum occurred in halogen-free melts with 57-60 wt.% SiO_2, but that the addition of F or Cl reduced zircon solubility.

By contrast, in metaluminous and peraluminous granites and pegmatites, typically the only Zr-Hf mineral is zircon (and rarely hafnon). The most common REE minerals are monazite and xenotime in low Ca metaluminous and peraluminous granites, and allanite in high Ca granites (Cuney and Friedrich, 1987), although A-type granites and NYF pegmatites may contain a wide variety of Y and REE minerals.

The solubility of zircon has recently been summarized elsewhere (Hanchar and Watson, 2003; Hoskin and Schaltegger, 2003) and therefore will only be discussed briefly here. Zircon solubility, as first noted by Watson (1979), is strongly dependent on temperature and melt composition, ranging from wt. % levels of Zr in peralkaline melts to <100 ppm Zr in siliceous metaluminous and peraluminous melts (depending on temperature). Zircon saturation can be described as a solubility product $[ZrO_2]\cdot[SiO_2]$. Zircon solubility is thus dependent on the SiO_2 content of the melt, and therefore, instead of using the ASI ratio as a melt compositional parameter, Watson and Harrison (1983) included SiO_2 in the denominator. Other network-modifying cations have subsequently been included, e.g., Baker et al. (2002), and a melt compositional parameter M can be defined as the molar ratio:

$$M = \frac{1}{Si} \text{x} \frac{Na + K + 2(Ca + Mg + Fe)}{Al} \quad (9)$$

Additional factors that affect zircon solubility are the F (Keppler, 1993) and Fe (Baker et al., 2002) contents of the melt, both of which increase zircon solubility. By contrast, the solubilities of zircon and hafnon decrease with increasing Li content of the melt (Linnen, 1998).

Ellison and Hess (1986), Linnen (1998) and Linnen and Keppler (2002) showed that the solubility of hafnon is always greater that that of zircon at the same pressure, temperature, and melt composition (Figure 9). However, the change in their relative solubilities with the ASI ratio of the melt is similar to that of manganocolumbite-manganotantalite. The molar zircon/hafnon solubility ratio in strongly peralkaline melts is close to unity, which means that zircon fractionation from such melts will have little effect on the Zr/Hf ratio of the residual melt. By contrast, the molar zircon/hafnon solubility ratio in a metaluminous melt at 800°C is approximately 0.2. This means that the fractional crystallization of zircon will deplete the melt in Zr relative to Hf and that the Hf content of zircon will increase with progressive crystallization. However, it should be noted that although some peraluminous granite

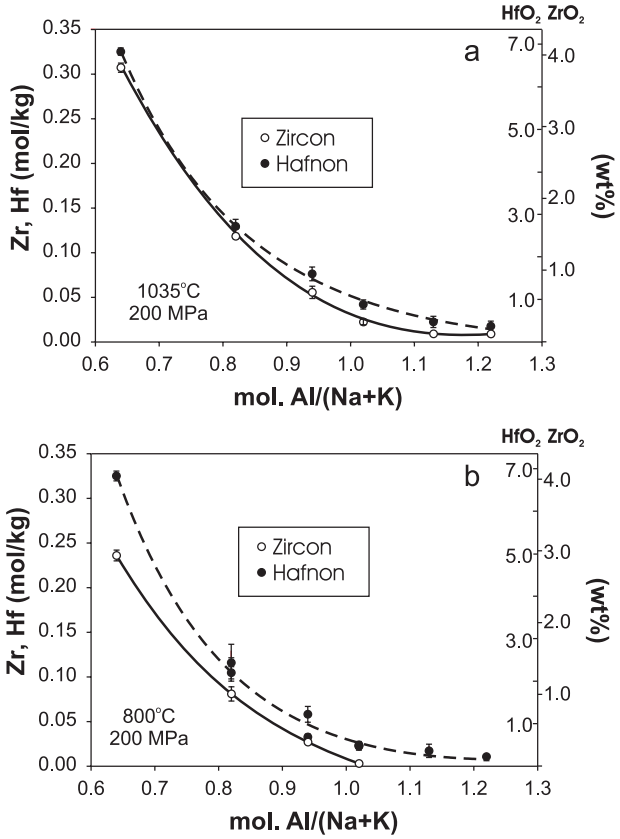

Figure 9. *Zircon-hafnon solubility in peralkaline to subaluminous haplogranitic melts at a) 1035°C and 200 MPa and b) 800°C and 200 MPa. The data is from Linnen and Keppler (2002).*

and rhyolite suites show a trend of decreasing Zr/Hf with increasing Hf (where Hf is an incompatible element this is a 'normal' magmatic trend) other suites show either a constant or increasing Zr/Hf with increasing Hf. Linnen and Keppler (2002) suggested that the latter behaviour could be explained by Hf being a compatible element in some cases, and the influence of restite zircon in other cases. Whether or not zircon can survive as a restite phase depends on the size of the zircon crystals as well as zircon solubility and Zr diffusivity in the melt (see Hanchar and Watson, 2003 for further discussion).

Monazite solubility in silicate melts has also been demonstrated to depend strongly on the ASI or M ratio of the melt as well as on temperature (Montel 1986; Rapp and Watson, 1986; Rapp et al., 1987; Ellison and Hess, 1988). It is evident that monazite solubility is very low in peraluminous melt compositions at the pressure-temperature conditions at which rare-element granites and pegmatites crystallize (Montel, 1993; Wolf and London, 1995). Total REE dissolved in monazite and H_2O-saturated silicate melts at 800°C range from > 1wt.% for low-silica, strongly peralkaline compositions, to a few hundred ppm for high-silica peraluminous compositions (Montel, 1993), to only a few tens of ppm for low temperature peraluminous rare-element granites. It has also been determined that the solubility of xenotime is greater than that of monazite in the same melt composition (Keppler, 1993; Wolf and London, 1995), and in the former study it was shown that solubilities increase from $LaPO_4$ to $GdPO_4$ to $YbPO_4$. However, in contrast to the solubilities of other high field strength elements, the F content of the melt has no effect on monazite or xenotime solubility (Keppler, 1993).

Sn and W Mineral Solubilities

Cassiterite is by far the most common Sn mineral. Most Sn deposits are hydrothermal in origin, but cassiterite in many pegmatites is interpreted to be magmatic in origin (e.g., Linnen and Williams-Jones, 1994). Experiments on cassiterite solubility in granitic melts have been conducted by Štemprok (1990), Taylor and Wall (1992), Linnen et al. (1995, 1996), Ellison et al. (1998), and Bhalla et al. (2005). Tin differs from the other rare-elements discussed above in that it can have different valences, Sn^{2+} and Sn^{4+}, at geologically relevant redox conditions. Cassiterite solubility increases dramatically with decreasing ASI values of peralkaline melts at both reduced (Linnen et al., 1996) and oxidized (Ellison et al., 1998) conditions. At reduced conditions, Linnen et al. (1996) observed that cassiterite solubility was at a minimum at the subaluminous (ASI=1.0) composition, then increased slightly with increasing ASI values of peraluminous melts (Figure 10). Bhalla et al. (2005) also observed an increase in cassiterite solubility with increasing ASI values of peraluminous melts, as well as increasing cassiterite solubility with increasing F and Cl contents of the melt. Taylor and Wall (1992), however, observed a decrease in cassiterite solubility with the addition of Cl to the melt. It is not clear why these latter two studies are in disagreement, although it may be related to problems with the experimental method that Taylor and Wall (1992) employed (see Linnen et al., 1995, for a discussion). Lastly, B has no apparent affect on the solubility of cassiterite (Wolf and London, 1994).

Oxygen fugacity is a major control of cassiterite solubility in subaluminous to peraluminous melt compositions: e.g., cassiterite saturation in H_2O-saturated subaluminous granitic melts at 850°C and 200 MPa ranges from 2.8 wt.% SnO_2 at a log f_{O_2} of FMQ-0.84 to ~800 ppm SnO_2 at FMQ+3.12 (where FMQ represents the fayalite-magnetite-quartz oxygen fugacity buffer; Linnen et al., 1995). The simple dissolution reaction illustrates that the log solubility of cassiterite should be proportional to -0.5 times the log f_{O_2}.

$$SnO_2^{crystal} = SnO^{melt} + 0.5O_2^{melt} \quad (10)$$

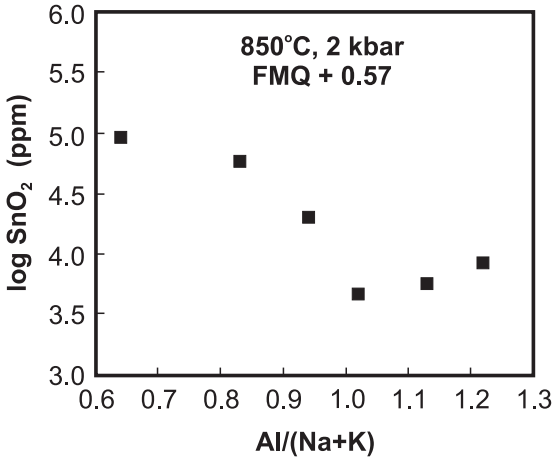

Figure 10. *Cassiterite solubility in peralkaline to peraluminous haplogranitic melts at 850°C and 200 MPa and a log f_{O_2} of FMQ+0.57, where FMQ represents the value at the fayalite-magnetite-quartz buffer. The data is from Linnen et al. (1996).*

Tin is dissolved in H_2O-saturated subaluminous to peraluminous melts dominantly as Sn^{2+} at log f_{O_2} conditions more reduced than ~ FMQ+2.5. By contrast, in strongly peralkaline granitic melts Sn^{4+} is the dominant valence of tin dissolved in the melt, even at log f_{O_2} conditions as reduced as the FMQ buffer (Linnen et al., 1996).

Štemprok (1990) and Bhalla et al. (2005) determined cassiterite solubility as a function of temperature. The temperature dependence of cassiterite solubility in the two studies was similar, although the absolute values were different because the melt compositions were different (Figure 11). One of the compositions was peralkaline and the f_{O_2} conditions were oxidizing (Štemprok, 1990), whereas the other set of experiments were conducted at f_{O_2} conditions where Sn^{2+} should dominate (Bhalla et al., 2005). The similarity of the temperature dependence of the two studies suggests that there is no significant enthalpy difference between SnO_2 dissolution as a Sn^{2+} or Sn^{4+} species in the melt. For a H_2O-saturated peraluminous melt with ~1 wt.% F and at a log f_{O_2} of Ni-NiO, Bhalla et al. (2005) derived the relationship:

$$\log C_{SnO_2} = 3.17 - 3510 / T \quad (11)$$

where C_{SnO_2} is the wt.% SnO_2 in the melt for cassiterite saturation and T is the temperature in Kelvin. This equation predicts that cassiterite saturation requires 1400 ppm SnO_2 at 600°C for this melt composition, but that lower SnO_2 abundances will result in cassiterite saturation at more oxidized conditions (Linnen et al., 1995, 1996).

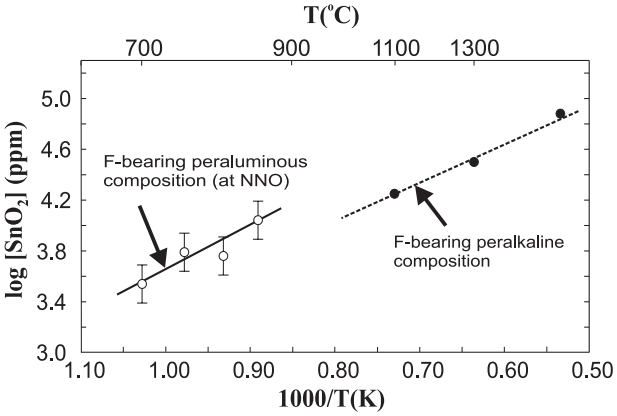

Figure 11. *Temperature dependence of cassiterite solubility in a natural F-rich granitic melt (Kymi topaz granite, Finland) and a synthetic F-rich peralkaline melt. The data is from Bhalla et al. (2005).*

The dominant ore minerals of W are scheelite and wolframite (ferberite-hübnerite solid solution). Wolframite is rare as a magmatic mineral (Tsareva et al., 1995) and we are not aware of any case where scheelite is reported to have crystallized directly out of a melt. Štemprok (1990) summarized the experimental work on WO_3 solubility in silicate melts. The solubility of hübnerite has been determined in a subaluminous granitic melt with variable Li contents (Linnen, 1998) and H_2O contents (Linnen, 2005). The hübnerite solubility product, $[MnO]\cdot[WO_3]$, in H_2O-saturated subaluminous granite melt at 200 MPa was not affected by Li and decreased from ~1.3x10^{-2} mol^2/kg^2 at 1035°C to ~5x10-4 mol^2/kg^{2}at 800°C (Linnen, 1998). The effect of melt ASI composition on hübnerite solubility is shown in Figure 12 (Linnen, unpublished data). The

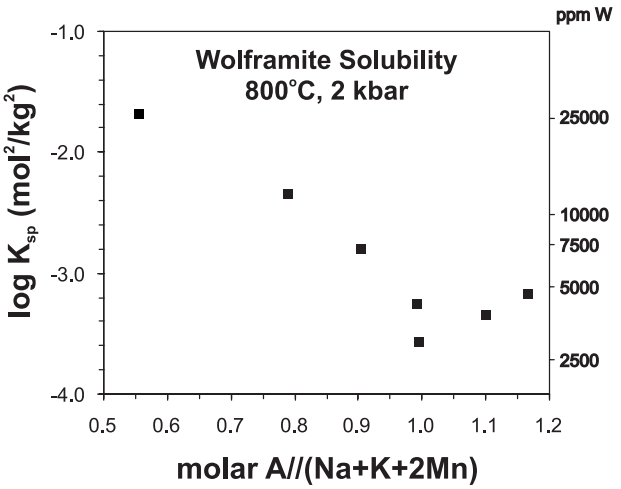

Figure 12. *Hübnerite solubility in peralkaline to peraluminous haplogranitic melts at 800°C and 200 MPa. The ppm W scale is based on stoichiometry dissolution/saturation of MnWO4.*

results are very similar to those for columbite-tantalite, with a solubility minimum at an ASI ratio of ~1.0, a strong increase in solubility with decreasing ASI values in peralkaline melts, and a weak increase in solubility with increasing ASI values in peraluminous melts. As is the case for columbite-tantalite, this also indicates that a few thousand ppm WO_3 are required for wolframite saturation in subaluminous to peraluminous granitic melts at 800°C.

Fluid-Melt Partitioning of Rare-Elements

There are only a few experimentally determined fluid-melt partition coefficients for rare-elements. It should be pointed out that the pH of the fluid wasn't controlled in any of these experiments, and since the solubilities of these elements are pH-dependent (Wood, this volume), this may affect fluid-melt partitioning (Frank et al., 2003; also see Samson and Wood, this volume). Two studies utilized natural glasses: London et al. (1988) used the peraluminous F-rich, Macusani glass at 775 to 435°C and 200 MPa, and Webster et al. (1989) used the peraluminous F-rich, Spor Mountain topaz rhyolite at 950 to 770°C and 50 to 400 MPa. The other studies cited below used synthetic granitic glasses as starting materials, and conducted experiments at 750 to 1000°C and 100 to 500 MPa. An exception is Keppler (1996), who studied haploandesite-H_2O and haploandesite-H_2O-(Na,K)Cl at 1040 to 1100°C and 0.3 to 2.0 GPa. The data from the Keppler (1996) study cannot be directly applied to granite-fluid systems but is included because of the lack of data for granitic systems.

It is important to note that in many studies the amount of Cl is varied because Cl is an important complexing agent for many elements. The partition coefficient of a rare-element thus will vary with the Cl content of the coexisting fluid if complexed as a chloride (cf. Candela and Piccoli, 1995). It is also worth noting that if the aqueous species of the rare-element is an oxyacid (e.g., W), an increase in its partitioning with the NaCl content of the fluid may be related to Na ion pairing rather than chlorine complexing (see the discussion on W below). Fluorine may complex rare-elements (Wood, this volume; Samson and Wood, this volume). However, F partitions in favour of the melt (London et al., 1988; Carroll and Webster, 1994; Chevychelov et al., 2004) and the F content of the

fluid has been varied in very few experimental studies. Overall, because of the preceding considerations, the fluid-melt partitioning of rare-elements is much less well understood compared to the solubilities of rare-elements in silicate melts.

Nb and Ta

London et al. (1988) determined that $D_{Nb}^{fluid–melt}$ is very low, ~0 to 0.1. Neither Keppler (1996) nor Schäfer et al. (1999) were able to determine $D_{Nb}^{fluid–melt}$ because of the low concentrations of Nb in the fluid. In F-bearing systems, Chevychelov et al. (2004) measured $D_{Nb}^{fluid–melt}$ values of ~0.005 to 0.008 at 100 MPa for peralkaline melt compositions. $D_{Nb}^{fluid–melt}$ values increased with decreasing temperature and with an increasing ASI ratio of the melt (note that F partitioning also depends on temperature and melt composition). Only in the study of Webster et al. (1989) did significant amounts of Nb partition into the fluid phase, thus partition coefficients from this study should be used with caution. They observed a complicated behaviour: $D_{Nb}^{fluid–melt}$ increased with decreasing pressure, increasing temperature, and with increasing Cl content of the fluid. At 200 MPa $D_{Nb}^{fluid–melt}$ was greater than 1.0 at temperatures over 850°C, but at 775°C was 0.2. A somewhat surprising result is that $D_{Nb}^{fluid–melt}$ was apparently dependent on the Cl concentration in the fluid. At 775 to 800°C and 200 MPa $D_{Nb}^{fluid–melt}$ increased from 0.2 to 3.3 for fluids with 0.16 and 2.96 *m* Cl, respectively. However, additional increases in the Cl content of the fluid, up to 6.13 *m*, did not change the $D_{Nb}^{fluid–melt}$ value, which suggests that Nb is not complexed by Cl and that the increase must be related to a different factor, such as ion pairing with alkalis or changes of pH.

Tantalum fluid-melt partition coefficients for peralkaline granitic systems have been measured in only one study, that of Chevychelov et al. (2004). The values of $D_{Ta}^{fluid–melt}$ are consistently lower than those of $D_{Nb}^{fluid–melt}$ from that study, and range from ~0.002 to 0.08. Chevychelov et al. (2004) also found that the temperature-dependence of $D_{Ta}^{fluid–melt}$ was greater than that of $D_{Nb}^{fluid–melt}$, and that $D_{Ta}^{fluid–melt}$ also increased with increasing ASI ratio in the melt. The only other study that attempted to measure $D_{Ta}^{fluid–melt}$ is that of Keppler (1996), where the concentrations of Ta in the aqueous fluids were below the detection limit, implying $D_{Ta}^{fluid–melt}$ <0.004 for haploandesite at the P-T conditions of the experiments. The lack of Ta enrichment in the geochemical aureoles above Ta-rich rare-element granites cupolas also supports an extremely low partition coefficient for Ta in the fluid phase, despite elevated Cl contents in the magmatic fluids, as observed for the Beauvoir granite and its mica schist envelope (Cuney et al., 1992).

Zr and Hf

We are aware of only one study that determined fluid-melt partition coefficients of Zr and Hf, that of London et al. (1988). In that study $D_{Zr}^{fluid–melt}$ ranged from ~0 to 0.2 and increased with decreasing temperature. $D_{Hf}^{fluid–melt}$ was slightly higher, ranging from ~0 to 0.7, and also increased with decreasing temperature, suggesting that Zr/Hf fractionation might be possible via hydrothermal processes.

Sn and W

The partition data for Sn is problematic because, at geologically relevant redox conditions, Sn is in either the 2+ or 4+ valence states in both silicate melts and aqueous fluids. Pure Sn melts at a low temperature (232°C) and under reducing conditions, cassiterite reacts with all of the precious metals that are used to make capsules to form alloys or tin-precious metal liquids that destroy the capsule (see Linnen et al., 1995). Consequently, the fluid-melt partition coefficients for Sn are very difficult to determine, particularly at reduced conditions. Taylor (1988) concluded that Sn is partitioned in favour of the melt when the chlorinity of the coexisting aqueous fluid is less than approximately 1 M at f_{O_2} conditions near that of the Ni-NiO buffer. Other studies (Nekrasov et al., 1980; Durasova et al., 1986; Keppler and Wyllie, 1991), report lower $D_{Sn}^{fluid–melt}$ values, 0.005 to 0.08 for 0 to 2 M HCl (starting fluid HCl contents). Keppler and Wyllie (1991) did not observed any effects of F on Sn partitioning and measured $D_{Sn}^{fluid–melt}$ values of ~0.1 to 0.2 for starting HF fluid concentrations of up to 3 M. In conclusion, only one study showed that significant amounts of Sn can be partitioned into a magmatic vapour phase, but given that Sn is readily complexed by Cl in aqueous solutions (Wilson and Eugster, 1990), it is expected that Sn will partition in favour of the fluid at high Cl concentrations. Until an experimental technique is developed that solves the problem of Sn reacting with precious metals, experimentally-derived fluid-melt partition coefficients for Sn should be used with caution.

Tungsten can also have different valences at geologically reasonable conditions (4+, 5+ and 6+). Candela and Bouton (1990) observed only a minor change in the silicate melt-ilmenite partition coefficient at different redox conditions, suggesting that W is dominantly at only one valence in granitic melts. Linnen (2005) further suggested that W^{6+} is the predominant valence in oxidized granitic melts (log f_{O_2}> NNO). However, it is also important to note that Ertel et al. (1996) determined that tungsten had a 4+ valence in an anhydrous haplobasaltic melt at 1300° to 1700°C over a log f_{O_2} range of ~10^{-15} to 10^{-9} bars (approximately FMQ-8 to FMQ-2). Tungsten also differs from Sn in that it forms an oxyacid complex, e.g., HWO_4^-, and as such can complex with alkalis, e.g., $NaHWO_4^0$ (Wood and Samson, 2000). There is some variation of fluid-melt partition coefficient values among the different experimental studies that have been published. For halogen-free studies, $D_W^{fluid–melt}$ ranges from 0.1 (Manning and Henderson, 1984), to ~ 4 (Schäfer et al., 1999) or ~5 (Keppler and Wyllie, 1991). Partitioning involving low salinity (NaCl) fluids also resulted in relatively high $D_W^{fluid–melt}$ values: 0.2 to 0.3 at 200 MPa (Kravchuk et al., 1997), ~0.3 to 1.0 at 100 MPa, and ~2.0 at 500 MPa (Chevychelov and Chevychelova, 1997). Keppler and Wyllie (1991) found that $D_W^{fluid–melt}$ decreased with the addition of HF or HCl and argued that this was due to the decrease of the fluid pH, as dictated by the following reaction:

$$WO_3^{melt} + H_2O^{fluid} = (WO_3(OH)^-)^{fluid} + (H^+)^{fluid} \quad (12)$$

Nonetheless, the $D_W^{fluid–melt}$ values from Keppler and Wyllie (1991) for coexisting HF or HCl fluids are relatively high, ~0.4 to 1.0. Bai and Koster van Groos (1999) observed decreasing $D_W^{fluid–melt}$ values with the addition of NaCl and a slight increase with the addition of HCl. By contrast, Manning and Henderson (1984) and Kravchuk et al. (1997) observed an increase of $D_W^{fluid–melt}$ with increasing NaCl or NaF in the fluid, but this increase could have been related to an increase in the pH of the coexisting fluid (Keppler and Wyllie, 1991). Bai and Koster van Groos (1999) also observed decreasing $D_W^{fluid–melt}$ values with the addition of $(Na,K)_2CO_3$, but it should also be pointed out that the addition of carbonate shifted the melt composition to highly peralkaline compositions.

REE

Partition coefficients have been determined by Flynn and Burnham (1978), London et al. (1988), Webster et al. (1989), Kravchuk et al. (1990), Bai and Koster van Groos (1999), and Reed et al. (2000). In

most studies where the concentration of Cl was a variable, $D_{REE}^{fluid-melt}$ increased with increasing Cl concentration in the fluid. The exception is Bai and Koster van Groos (1999) who observed increasing $D_{REE}^{fluid-melt}$ with increasing HCl concentration in the fluid, but no effect with increasing (Na,K)Cl concentration in the fluid. These results indicate that the REE are complexed as chlorides, and, because the fluid-melt partitioning of Cl is a complex function of temperature, pressure and melt composition (Carroll and Webster, 1994), $D_{REE}^{fluid-melt}$ will be similarly complex. Reed et al. (2000) determined that the $D_{REE}^{fluid-melt}$ values are all <0.01 at 800°C and 200 MPa for their experiments with an initial Cl^- concentration in the fluid of 0.4 m. There was also a decrease in $D_{REE}^{fluid-melt}$ with increasing atomic number of the REE. As the salinity of the initial fluid increased, $D_{REE}^{fluid-melt}$ increased, and at $[Cl^-]_{fluid}$ of 3.5 m, $D_{REE}^{fluid-melt}$ for the LREE was >1.0.

DISCUSSION

Temperature and Pressure of Ta-Nb-Sn Mineralization

The pressure at which Ta-Nb-Sn mineralization occurs can be constrained by the metamorphic assemblages of the rocks into which the pegmatites and granites intruded, by the lithium silicate mineral assemblage (petalite-spodumene; e.g., London, 1986), or by using fluid inclusions. Granite-hosted deposits are typically emplaced at a very high level, commonly sub-volcanic, whereas LCT pegmatites are generally emplacement at moderate pressures, 300-500 MPa.

The temperature at which columbite-tantalite crystallizes in natural pegmatites and granites is poorly constrained, and is based primarily on fluid inclusion and melt inclusion data, silicate mineral phase equilibria and liquidus-solidus temperatures from experiments on granitic systems. Fluid inclusion estimates of crystallization temperatures of natural pegmatites range considerably. The highest temperature of tantalite crystallization reported in the literature is 750°C at 500 MPa, interpreted for the strongly deformed Greenbushes pegmatite (Partington et al., 1995). These values are difficult to evaluate because they are based on fluid inclusion data that were not included in that paper. Petalite at the Tanco pegmatite initially crystallized at ~600°C and 325 MPa, but lower temperatures are estimated for the crystallization temperatures of the Ta-mineralized units, from 600° to <400°C at ~300 to 270 MPa (London, 1986; Morgan and London, 1987; Thomas et al., 1988, 1990; see also Černý, this volume). The Nong Sua Sn-W-Nb-Ta pegmatite in Thailand is estimated to have crystallized at ~650°C and 380 MPa (Linnen and Williams-Jones, 1994). The magmatic stage of the Harding pegmatite, New Mexico, includes the crystallization of tantalite at 650° to 550°C at 330 to 350 MPa (Chakoumakos and Lumpkin, 1990). Beurlen et al. (2001) observed primary aqueous-carbonic inclusions in manganotantalite from the Borborema Province, northeast Brazil, and concluded that these fluids were trapped at ~580°C and 350 MPa. The minimum P-T conditions for the Forcarei Sur rare element pegmatite field in Galicia, Spain is 550°C and 300 MPa (Fuertes-Fuente and Martin-Izard, 1998). Considerably lower temperatures, 350°-400°C at 270 MPa, are estimated for the crystallization temperature of the Tin Mountain pegmatite (Sirbescu and Nabelek, 2003).

Solidus temperatures for granitic melts rich in fluxing agents (F, B, Li, P) are similar to the temperature estimates of Ta mineralization discussed above: ~600°C at 200 MPa for the Li-rich Harding pegmatite (Burnham and Nekvasil, 1986); ~700° to 650°C at 100 to 300 MPa for the B-rich HIM-3 granite (Benard et al., 1985); ~580° to 550°C at 100 to 300 MPa for the Li-F-P-rich the Beauvoir granite (Pichavant et al., 1987a). The Spor Mountain vitrophyre, which contains 1.2 wt. % F, also has a very low solidus temperature, ≤550°C (Webster et al., 1987). Other relevant experiments include the fluxing effects of P_2O_5 (London et al., 1993) and Li_2O (Stewart, 1978; Chou and Anderson, 1998). The lowest experimentally determined liquidus and solidus temperatures for granitic melts are those of the Macusani glasses (London et al., 1989). This natural glass, which is rich in Li, P, B and Li has, at 200 MPa, liquidus temperatures of ~950° to 600°C, depending on H_2O content, and a solidus temperature of ~450°C. Remelting of melt inclusions also provides direct information on the solidus and liquidus temperature of rare-element granitic melts, with similar estimates to those listed above (e.g., Webster et al., 1997; Thomas et al., 1996 and 2000; Badanina et al., 2004).

Magmatic Mineralization

Deciphering source melting mechanisms, and the observed or inferred degree of fractionation of rare-element-enriched magmas, are key for understanding the genesis of the associated rare-element deposits. Crystal fractionation appears to be the most important mechanism leading to rare-element enrichment (Congdon and Nash, 1991; Černý, 1991b; Raimbault et al., 1995). In some cases, rare-element fractionation can be traced from less to more fractionated granite phases, suggesting that the source granites may be derived from source rocks with average rare-element abundances (e.g., Lehmann, 1990). If the source granites contain Ta abundances close to, or lower than, 1 ppm (see Table 1), a degree of fractionation lower than 0.01 is required for the most fractionated rare-element granites to attain Ta concentrations on the order of several hundreds of ppm. This corresponds to less than 1 wt.% of residual silicate melt fraction in a perfect fractional crystallization model. However, in rare-element granite complexes, less-fractionated phases may be absent, diachronous, or cannot be simply related by fractional crystallization to the spatially related rare-element granite body. Derivation of rare-element granites from a very low degree of partial melting in the lower or middle crust (Christiansen et al., 1986; Manning and Hill, 1990; Pichavant et al., 1987b) or from partial melting of sources enriched in rare-elements (Cuney et al., 1992; Marignac and Cuney, 1999), or a combination of partial melting and crystal fractionation (e.g., Burt et al., 1982), have also been proposed. If Ta contents are used as a reference to estimate the degree of magma fractionation, the enrichments of Sn, W, Rb, Li, etc. that are observed in different rare-element granites indicate that they share a similar geochemical signature (Figure 4). However, variations in different element ratios could reflect variable degree of enrichment of these elements in the source material that was partially melted, differences in the nature or abundance of the phases crystallized, or differences in oxygen fugacity.

The available mineral-melt partition data suggests that the Ta, Nb, Sn, and W concentrations in granitic melts are controlled dominantly by the crystallization of Ti-rich minerals, notably titanite and magnetite. Consequently, these elements are the most incompatible in granites that have the lowest modal abundances of these minerals, i.e., reduced, S-type and/or ilmenite-series granitic rocks. The alternate explanation to extreme fractionation for high rare-element concentrations is very low degrees of partial melting, as was discussed above. In this case, the mineral-melt partition data indicates that the most favourable source would be one rich in Ti min-

erals, i.e., titanite, magnetite and/or rutile (assuming that these minerals do not remain as restite).

The temperatures of Ta mineralization in general overlap with the crystallization temperatures of granitic melts rich in fluxing elements, with which they are associated. In rare-element granites, columbite-tantalite and microlite occur homogeneously disseminated within the major rock-forming minerals with no evidence of vein type distribution. These minerals have locally been observed as inclusions in the same quartz that bears melt inclusions and even in the melt inclusions themselves. All of these features indicate a magmatic origin for Ta mineralization. Tantalite in LCT pegmatites is commonly in layers in saccharoidal albite units, but also can be associated with intermediate pegmatite zones, where it also can be intergrown with K-feldspar, muscovite, and/or lepidolite (e.g., at Tanco; Ercit, 1986). The mineralization in the albite units is synchronous with the albite, and the latter is generally interpreted to be magmatic in origin, although layers of nearly pure albite may result from a process such as constitutional zone refining (e.g., London, this volume). Oscillatory growth bands (e.g., Lahti, 1987) are probably magmatic in origin, with sharp breaks in Ta/Nb ratio, possibly in response to very slow Nb and Ta diffusion in silicate melt (Mungall et al., 1999). However, very complicated compositions or evidence of replacement textures are also commonly observed, which indicate, at least in part, a hydrothermal origin. The origin of these patterns is, however, poorly understood. Compositional variation could be the result of direct deposition from hydrothermal fluids, but also could result from local remobilization of Nb or Ta from primary magmatic oxides (i.e., the Ta and Nb may only move very short distances, but the resulting zonation in the crystals will be complex).

The relationship between Ta mineralization and fluxing elements, Li-F in particular, is paradoxical because the addition of fluxing elements to a granitic melt increases tantalite solubility (Figure 8). At 600°C, several thousand ppm Ta are required for tantalite saturation in a melt with 2 wt.% F, which probably is an unreasonably high value considering that the parental melt likely initially has only on the order of 1 ppm Ta. The highest amount of Ta observed in a natural glass or melt inclusion is 521 ppm (Webster et al., 1997), but this may result from the fact that the natural examples were not tantalite-saturated, and Ta contents increase during fractionation. An additional explanation is the possible competing effects between the variety of rare elements that are present in natural melts. The paradox is that at lower temperatures tantalite solubility will be lower, however, the amount of fluxing elements in the melt, required to attain lower solidus temperatures, also increases tantalite solubility. Two possible solutions to this paradox are: 1) If the Li and F contents of the melt are lowered via crystallization of a phase such as petalite, or lepidolite, the solubility product of tantalite will be lowered (less soluble in a flux-free melt), which could trigger tantalite saturation (in this case <1000 ppm Ta in the melt required; Linnen, 1998); 2) the granitic magmas are strongly supercooled and the crystallization of tantalite is possible because of the very low temperature of the magma (London, this volume). It is interesting that the addition of F to silicate melts increases the amount of undercooling that a silicate melt can attain (see London, 2005b, and the references therein). With the exception of the fluid inclusion study by Beurlen et al. (2001), the temperatures of tantalite crystallization are in fact poorly constrained, e.g., at Tanco temperatures are based on fluid inclusions in quartz or spodumene or on lithium silicate phase equilibria, neither of which, in detail, are directly associated with the Ta mineralization. More detailed studies that focus specifically on Ta mineralization are required to better establish the temperature of mineralization, which is needed to test the supercooling model.

Magmatic-Hydrothermal Mineralization

There are several lines of evidence that suggest that Ta mineralization is not hydrothermal in origin. Ta haloes are lacking around rare-element pegmatites, although the wallrocks surrounding the pegmatites are typically enriched in alkalis, e.g., Li, Rb and Cs, which can be used as an exploration tool (Galeschuk and Vanstone, this volume). In plutonic rocks, Ta mineralization appears to be magmatic, but the presence of late- to post-magmatic alteration that is rich in volatile elements (particularly F) makes it difficult to separate the effects of magmatic fractionation from fluid/rock interactions. A redistribution of the rare-element mineralization in some deposits by late-magmatic, F-rich fluids within the granitic intrusion has been proposed for some deposits (e.g., Pollard et al., 1989a,b). However, these studies do not demonstrate the extent to which the hydrothermal transport of the rare-elements has contributed to the enrichment of the ore deposits. Where the fluids escape into the enclosing rocks, skarn, breccia, and vein-type mineralization may occur. But the mineralization related to these fluids is mainly cassiterite and/or wolframite, with very limited Ta and Nb substitutions. For example, the mica schist at the roof of the Beauvoir rare-element granite is strongly enriched in Sn, W, F, Li, and Rb, but not Ta. The concentrations of Nb and Ta in the mica schist are dramatically lower than the granite at the top of the cupola (Cuney et al., 1992). This implies that Ta was not transported by aqueous (± carbonic) fluids, which is consistent with the very low fluid-melt partition coefficients that have been reported. It is interesting that Nb can be enriched in the surrounding wallrock and that this element has a higher fluid-melt partition coefficient than Ta, which suggests that Nb may be more mobile. The fluid-melt partition coefficients for Sn and W are significantly higher than those for Nb or Ta, and Sn-W mineralization can be magmatic-hydrothermal in origin as well as magmatic in rare-element granitic systems, as shown by their common occurrence as vein type deposits. This is consistent with the observation that most Sn-W deposits that lack Nb and Ta are magmatic-hydrothermal in origin, rather than magmatic, Lehmann (1990).

Badanina et al. (2004) used homogenized melt inclusions to demonstrate immiscibility between a K-rich aluminosilicate melt and a Na-F-rich hydrosaline melt in the most evolved units of the Orlovka granite complex, a phenomena also supported by the results of experimental studies (Veksler et al., 2002, and this volume). Similarly, complete miscibility between silicate melts and hydrous fluids at low pressure and relatively low temperature was interpreted in the melt inclusion study of the F-B-P-rich Ehrenfriedensdorf pegmatite (Thomas, et al., 2000). However, the experimental data of Sowerby and Keppler (2002) indicate a temperature of >600°C for supercritical behaviour at 200 MPa for a melt with very high concentrations of fluxing elements. The role of immiscibility on the distribution of rare-elements in highly evolved granites and pegmatites for both natural and experimentally derived samples remains enigmatic. However, it is very important for future studies to determine whether this is an important process for the formation of rare-element deposits.

ACKNOWLEDGMENTS

Many of the experiments discussed in this chapter benefited from input by Hans Keppler, David London and Michel Pichavant. The

chapter also was improved by reviews from Bernd Lehmann, Iain Samson and Michael Wolf. Lastly, I would like to thank Steve Piercey and the Mineral Deposits Division of the Geological Association of Canada for the opportunity of holding this short course.

REFERENCES

Antipin, V.S., Kovalenko, V.I., Kuznetsova, A.I., and Persikova, L.A., 1981, Distribution coefficients for tin and tungsten in ore-bearing acid igneous rocks: Geochemistry International, v. 18, no. 1, p. 92-106.

Badanina, E.V., Veksler, I.V., Thomas, R., Syritso, L.F., and Trumbull, R.B., 2004, Magmatic evolution of Li-F, rare metal granites: a case study of melt inclusions in the Khangilay complex, Eastern Transbaikalia (Russia): Chemical Geology, v. 210, p. 113-133.

Bai, T.B., and Koster van Groos, A.F., 1999, The distribution of Na, K, Rb, Sr, Al, Ge, Cu, W, Mo, La, and Ce between granitic melts and coexisting aqueous fluids: Geochimica et Cosmochimica Acta, v. 63, p. 1117-1131.

Baker, D.R., Conte, A.M., Freda, C., and Ottolini, L., 2002, The effect of halogens on Zr diffusion and zircon dissolution in hydrous metaluminous granitic melts: Contributions to Mineralogy and Petrology, v. 142, p. 666-678.

Bea, F., 1996, Residence of REE, Y, Th and U in granites and crustal protoliths; Implications for the chemistry of crustal melts: Journal of Petrology, v. 37, p. 521-552.

Benard, F., Moutou, P., and Pichavant, M., 1985, Phase relations of tourmaline leucogranites and the significance of tourmaline in silicic melts: Journal of Geology, v. 93, p. 271-291.

Beurlen, H., da Silva, M.R.R., and de Castro, C., 2001, Fluid inclusion microthermometry in Be-Ta-(Li-Sn)-bearing pegmatites from the Borborema Province, Northeast Brazil: Chemical Geology, v. 173, p. 107-123.

Beus, A.A., 1982, Metallogeny of Precambrian rare-metal granitoids: Rev. Bras. Geosci., v. 12, p. 410-413.

Beus, A.A., Severov, V.A., Sitnin, A.A., and Subbotin, K.D., 1962, Albitized and greisenized granites (apogranites): Moscow, Akademiia Nauk SSSR, 196 p. (in Russian).

Beus, A.A., and Zhalashkova, N.Y., 1964, Postmagmatic high temperature metasomatic processes in granitic rocks: International Geology Review, v. 6, p. 668-681.

Bhalla, P., Holtz, F., Linnen, R.L., and Behrens, H., 2005, Solubility of cassiterite in evolved granitic melts; effect of T, f_{O_2} and additional volatiles: Lithos, v. 80, p. 387-400.

Bothelo, N.F., and Moura, M.A., 1998, Granite-ore deposit relationships in central Brazil: Journal of South American Earth Sciences, v. 11, p. 427-438.

Breaks, F.W., Selway, J.B., and Tindle, A.G., 2005, Fertile peraluminous granites and related rare-element pegmatite mineralization, Superior Province of Ontario: *in* Linnen, R.L., and Samson, I.M., eds., Rare-Element Geochemistry and Mineral Deposits, Geological Association of Canada Short Course Notes, v. 17, p. 87-125.

Breiter, K., 1998, Genetic significance of phosphorus in fractionated granites: Excursion guide, Czeck Geological Survey, Prague, 170 p.

Burnham, C.W., and Nekvasil, H., 1986, Equilibrium properties of granite pegmatite magmas: American Mineralogist, v. 71, p. 239-263.

Burt, D.M., Sheridan, M.F., Bikun, J.V., and Christiansen, E.H., 1982, Topaz rhyolites - distribution, origin, and significance for exploration: Economic Geology, v. 77, p. 1818-1836.

Candela, P.A., and Bouton, S.L., 1990, The influence of oxygen fugacity on tungsten and molybdenum partitioning between silicate melts and ilmenite: Economic Geology, v. 85, p. 633-640.

Candela, P.A., and Piccoli, P., 1995, Model ore-metal partitioning from melts into vapor and vapor/brine mixtures: *in* Thompson, J.F.H., ed., Magmas, Fluids, and Ore Deposits, Mineralogical Association of Canada Short Course, v. 23, p. 101-127.

Carroll, M.R., and Webster, J.D., 1994, Solubilities of sulfur, noble gases, nitrogen, chlorine, and fluorine in magmas: *in* Carroll, M.R., and Holloway, J.R., eds., Volatiles in Magmas, Mineralogical Society of America, Reviews in Mineralogy, v. 30, p. 231-279.

Černý, P., 1991a, Rare-element granitic pegmatites. Part I: Anatomy and internal evolution of pegmatite deposits: Geoscience Canada, v. 18, p. 49-67.

Černý, P., 1991b, Fertile granites of Precambrian rare-element pegmatite fields: Is geochemistry controlled by tectonic setting or source lithologies?: Precambrian Research, v. 51, p. 429-468.

Černý, P., 2005, The Tanco rare-element pegmatite deposit, Manitoba: Regional context, internal anatomy, and global comparisons: *in* Linnen, R.L., and Samson, I.M., eds., Rare-Element Geochemistry and Mineral Deposits, Geological Association of Canada Short Course Notes, v. 17, p. 127-158.

Černý, P., and Ercit, T. S., 1985, Some recent advances in the mineralogy and geochemistry of Nb and Ta in rare-element granitic pegmatites: Bulletin Minéralogie, v. 108, p. 499-532.

Černý, P., and Ercit, T.S., 1989, Mineralogy of niobium and tantalum: Crystal chemical relationships, paragenetic aspects and their economic implications: *in* Möller, P., Černý, P., and Saupé, F., eds., Lanthanides, Tantalum and Niobium, Springer-Verlag, Berlin, p. 27-79.

Černý, P., Ercit, T.S., and Vanstone, P.J., 1998, Mineralogy and petrology of the Tanco rare-element pegmatite deposit, southeastern Manitoba: International Mineralogical Association Fieldtrip Guidebook B6, 74 p.

Černý, P., Goad, B.E., Hawthorne, F.C., and Chapman, R., 1986, Fractionation trends of the Nb- and Ta-bearing oxide minerals in the Greer Lake pegmatitic granite and its pegmatite aureole, Southeastern Manitoba: American Mineralogist, v. 71, p. 501-517.

Černý, P., and Nemec, D., 1995, Pristine vs. contaminated trends in Nb, Ta-oxide minerals of the Jihlava pegmatite district, Czech Republic: Mineralogy and Petrology, v. 55, p. 117-129.

Chakoumakos, B.S., and Lumpkin, G.R., 1990, Pressure-temperature constraints on the crystallization of the Harding pegmatite, Taos County, New Mexico: Canadian Mineralogist, v. 28, p. 287-298.

Charoy, B., and Noronha, F., 1996, Multistage growth of a rare-element, volatile-rich microgranite at Argemela (Portugal): Journal of Petrology, v. 37, p. 73-94.

Cheilletz, A., Bertrand, J.M., Charoy, B., Moulahoum, O., Bouabsa, L., Farrar, E., Zimmermann, J.L., Dautel, D., Archibald, D.A., and Boullier, A.M., 1992, Géochimie et géochronologie Rb-Sr, K-Ar et $^{40}Ar/^{39}Ar$ des complexes granitiques Pan-africains de la région de Tamanrasset (Algérie): relations avec les minéralisations Sn - W associées et l'évolution tectonique du Hoggar central: Bull. Société Géologique France, v. 163, p. 733-750.

Chevychelov, V.Yu., and Chevychelova, 1997, Partitioning of Pb, Zn, W, Mo, Cl and major elements between aqueous fluid and melt in the systems granodiorite (granite, leucogranite)-H_2O-NaCl-HCl: N. Jb. Mineral. Abh, v. 172, p. 101-115.

Chevychelov, V.Yu., Zaraisky, G., Borisovsky, S., and Borkov, D., 2004, Partitioning of Ta and Nb between magmatic melt and

aqueous (K,Na,H)F-containing fluid: Effects of temperature and chemical composition of the melt: EMPG-X Symposium Abstracts, Lithos supplement to v. 73, Nos. 1-2, p. S17.

Chou, I.-M., and Anderson, A.J., 1998, Direct observation of low temperature melting in the system petalite-quartz-H_2O using a hydrothermal diamond anvil cell: Methods and geological interpretation: Goldschmidt Conference Abstracts, Mineralogical Magazine, v. 62a, p. 327-328.

Christiansen, E.H, Sheridan, M.F., and Burt, D.M., 1986, The geology and geochemistry of Cenozoic topaz rhyolites from the western United States: Geological Society of America Special Paper 205, 82 p.

Congdon, R.D., and Nash, W.P., 1991, Eruptive pegmatite magma: Rhyolite of the Honeycomb Hills, Utah: American Mineralogist, v. 76, p. 1261-1278.

Cuney, M., and Autran, A., 1987, Le forage scientifique d'Echassières (Allier). Une clé pour la compréhension des mécanismes magmatiques et hydrothermaux associés aux granites à métaux rares: Mémoire GPF, Géologie de la France, v. 1, 350 p.

Cuney, M., and Friedrich, M., 1987, Physicochemical and crystal-chemical controls on accessory mineral paragenesis in granitoids. Implications on uranium metallogenesis: Bulletin Minéralogie, v. 110, p. 235-247.

Cuney, M., Marignac, C., and Weisbrod, A., 1992, The Beauvoir topaz-lepidolite albitic granite (Massif Central France). A highly specialized granite with disseminated Sn-Li-Ta-Nb-Be mineralization of magmatic origin: Economic Geology, v. 87, p. 1766-1794.

Dingwell, D.B., 1988, The structures and properties of fluorine-rich magmas: a review of experimental studies: *in* Taylor, R.P., and Strong, D.F., eds., Recent Advances in the Geology of Granite Related Mineral Deposits: Canadian Institute of Mining and Metallurgy, Special Volume 39, p. 1-12.

Durasova, N.A., Ryabchikov, I.D., and Barsukov, V.L., 1986, The redox potential and the behaviour of tin in magmatic systems: International Geological Review, v. 28, p. 305-311.

Eby, G.N., 1992, Chemical subdivision of the A-type granitoids: Petrogenetic and tectonic implications: Geology, v. 20, p. 641-644.

Ellison, A.J.G., and Hess, P.C., 1986, Solution behavior of +4 cations in high silica melts: petrologic and geochemical implications: Contributions to Mineralogy and Petrology, v. 94, p. 343-351.

Ellison, A.J.G., and Hess, P.C., 1988, Peraluminous and peralkaline effects upon "monazite" solubility in high-silica liquids: EOS, v. 69, no. 16, p. 498.

Ellison, A.J.G., Hess, P.C., and Naski, G.C., 1998, Cassiterite solubility in high-silica K_2O-Al_2O_3-SiO_2 liquids: Journal of the American Ceramic Society, v. 81, p. 3215-3220.

Ercit, T.S., 1986, The simpsonite paragenesis; the crystal chemistry and geochemistry of extreme Ta fractionation: PhD Thesis, University of Manitoba, Winnipeg, Manitoba, 471 p.

Ercit, T.S., 2005, REE-enriched granitic pegmatites: *in* Linnen, R.L., and Samson, I.M., eds., Rare-Element Geochemistry and Mineral Deposits, Geological Association of Canada Short Course Notes, v. 17, p. 175-199.

Ercit, T.S., Černý, P., Hawthorne, F.C., and McCammon, C.A., 1992, The wodginite group. II. Crystal chemistry: Canadian Mineralogist, v. 30, p. 613-631.

Ertel, W., O'Neill, H.St.C, Dingwell, D.B., and Spettel, B., 1996, Solubility of tungsten in a haplobasaltic melt as a function of temperature and oxygen fugacity: Geochimica et Cosmochimica Acta, v. 60, p. 1171-1180.

Ewing, R.C., and Chakoumakos, B.C., 1982, Lanthanide, Y, Th, U, Zr and Hf minerals: selected structure descriptions: *in* Černý, P., ed., Granitic Pegmatites in Science and Industry, Mineralogical Association of Canada Short Course, v. 8, p. 239-265.

Fetherstone, J.M., 2004, Tantalum resources in Western Australia: Geological Survey of Western Australia, Mineral Resources Bulletin 22, 162 p.

Flynn, R.T., and Burnham, C.W., 1978, An experimental determination of rare earth partition coefficients between a chloride containing vapor phase and silicate melts: Geochimica et Cosmochimica Acta, v. 42, p. 685-701.

Foord, E.E., 1982, Minerals of tin, titanium, niobium and tantalum in granitic pegmatites: *in* Černý, P., ed., Granitic Pegmatites in Science and Industry, Mineralogical Association of Canada Short Course, v. 8, p. 187-238.

Forsythe, L.M., Nielsen, R.L., and Fisk, M.R., 1994, High-field-strength element partitioning between pyroxene and basaltic to dacitic magmas: Chemical Geology, v. 117, p. 107-125.

Frank, M.R., Candela, P.A., and Piccoli, P.M., 2003, Alkali exchange equilibria between a silicate melt and coexisting magmatic volatile phase: An experimental study at 800°C and 100 MPa: Geochimica et Cosmochimica Acta, v. 67, p. 1415-1427.

Fuertes-Fuente, M., and Martin-Izard, A., 1998, The Forcarei Sur rare-element granitic pegmatite field and associated mineralization, Galicia, Spain: Canadian Mineralogist, v. 36, p. 303-325.

Gagny, C., 1987, Organisation séquentielle évolutive des intrusions successives du granite de Beauvoir dans son caisson: arguments géochimiques: *in* Cuney M., and Autran A., eds., Echassières: le forage scientifique. Une clé pour la compréhension des mécanismes magmatiques et hydrothermaux associés aux granites à métaux rares: Géologie de la France, v. 2-3, p. 199-208.

Galeschuk, C.R., and Vanstone, P.J., 2005, Exploration for buried rare-element pegmatites in the Bernic Lake area of southeastern Manitoba: *in* Linnen, R.L., and Samson, I.M., eds., Rare-Element Geochemistry and Mineral Deposits, Geological Association of Canada Short Course Notes, v. 17, p. 159-173.

Gramenitskiy, E.N., and Shchekina, T.I., 2001, On the geochemistry of Ta, Nb, Zr, and Hf in F-enriched granites and alkaline rocks: Experimental data: Geochemistry International, v. 39, p. 563-576.

Green, T.H., Blundy, J.D., Adam, J., and Yaxley, G.M., 2000, SIMS determination of trace element partition coefficients between garnet, clinopyroxene and hydrous basaltic liquids at 27.5 GPa and 1080-1200°C: Lithos, v. 53, p. 165-187.

Green, T.H., and Pearson, N.J., 1987, An experimental study of Nb and Ta partitioning between Ti-rich minerals and silicate liquids at high pressure and temperature: Geochimica et Cosmochimica Acta, v. 51, p. 55-62.

Hanchar, J.M., and Watson, E.B., 2003, Zircon saturation thermometry: *in* Hanchar, J.M., and Hoskin, P.W.O., eds., Zircon, Reviews in Mineralogy and Geochemistry, v. 53, p. 89-112.

Hildreth, W.E., 1979, The Bishop Tuff: Evidence for the origin of the compositional zonation in silicic magma chambers: Geological Society of America Special Paper 180, p. 43-76.

Hill, E., Wood, B.J., and Blundy, J.D., 2000, The effect of Ca-Tschermaks component on trace element partitioning between clinopyroxene and silicate melt: Lithos, v. 53, p. 203-215.

Horng, W.S., and Hess, P.C., 1995, Results of HFS element (Ti, Nb, and Ta) saturation and dissolution experiments in water-saturated Macusani glasses: EOS, v.76, no. 46, p. F648.

Horng, W.S., and Hess, P.C., 2000, Partition coefficients of Nb and Ta between rutile and anhydrous haplogranite melts: Contributions to Mineralogy and Petrology, v. 138, p. 176-185.

Hoskin, P.W.O., and Schaltegger, U., 2003, The solubility of zircon and igneous and metamorphic petrogenesis: *in* Hanchar, J.M., and Hoskin, P.W.O., eds., Zircon, Reviews in Mineralogy and Geochemistry, v. 53, p. 27-62.

Hu, S., Sun, M., Yan, Z., Xu, J., Cao X., and Ye, Y., 1984, An important metallogenetic model for W, Sn and rare granitophile elements ore deposits related to metasomatically altered granites: Geology of Granites and Their Metallogenetic Relations. International Symposium, Nanjing University, Nanjing, October 26-30, 1982, Proceedings, p. 519-537.

Ishihara, S., 1981, The granitoids series and mineralization: Economic Geology 75th Anniversary Volume, p. 458-484.

Jacquot, T., and Gagny, C., 1987, Pétrologie structurale du granite de Beauvoir : données et interprétation à son niveau apical: *in* Cuney, M., and Autran, A., eds., Echassières: le forage scientifique. Une clé pour la compréhension des mécanismes magmatiques et hydrothermaux associés aux granites à métaux rares : Géologie de la France v. 2-3, p. 57-62.

Keppler, H., 1993, Influence of fluorine on the enrichment of high field strength trace elements in granitic rocks: Contributions to Mineralogy and Petrology, v. 114, p. 479-488.

Keppler, H., 1996, Constraints from partitioning experiments on the composition of subduction-zone fluids: Nature, v. 380, p. 237-240.

Keppler, H., and Wyllie, P.J., 1991, Partitioning of Cu, Sn, Mo, W, U, and Th between melt and aqueous fluid in the systems haplogranite-H_2O-HCl and haplogranite-H_2O-HF: Contributions to Mineralogy and Petrology, v. 109, p. 139-150.

King, P.L., Chappell, B.W., Allen, C.M., and White, A.J.R., 2001. Are A-type granites the high temperature felsic granites? Evidence from fractionated granites of the Wangrah Suite: Australian Journal of Earth Science, v. 48, p. 501-514.

King, P.L., White, A.J.R., Chappell, B.W., and Allen, C.M., 1997. Characterization and origin of aluminous A-type granites from the Lachlan Fold Belt, Southeastern Australia: Journal of Petrology, v. 38, p. 371-391.

Kinnaird, J.A., Bowden, P., Ixer, R.A., and Odling, N.W.A., 1985, Mineralogy, geochemistry and mineralization of the Ririwai complex, northern Nigeria: Journal of African Earth Science, v. 3, p. 185-222.

Klein, M., Stosch, H.G., and Seck, H.A., 1997, Partitioning of high field-strength and rare-earth elements between amphibole and quartz-dioritic to tonalitic melts: an experimental study: Chemical Geology, v. 138, p. 257-271.

Kontak, D.J., 1990, The East Kemptville topaz-muscovite leucogranite. I. Geological setting: Canadian Mineralogist, v. 28, p. 787-825.

Kovalenko, V.I., 1978, The genesis of rare metal granitoids and related ore deposits: *in* Štemprok, M., Burnol, and Tischendorf, G., eds., Metallization Associated with Acid Magmatism, Geological Survey, Prague, v. 3, p. 235-258.

Kovalenko, V.I., Antipin, V.S., Konusova, V.V., Smirnova, Ye.V., Petrov, L.L., Vladykin, N.V., Kuznetsova, A.I., Kostyukova, Ye.S., and Pisarskaya, V.A., 1977, Partition coefficients of fluorine, niobium, tantalum, lanthanum, ytterbium, yttrium, tin and tungsten in Ongonite: Doklady Earth Science, v. 233, p. 203-205.

Kovalenko, V.I., and Kovalenko, N.I, 1976, Ongonites (topaz bearing quartz keratophyre) – subvolcanic analogues of rare metal Li-F granites: Nauka, Moskva, 124 p. (in Russian).

Kovalenko, V.I., Kuz'min, M.I., and Letnikov, F.A., 1970, Magmatic origin of lithium and fluorine bearing rare metal granites: Doklady Akademii Nauk SSSR, Earth Sciences Section, v. 190, p. 189-192.

Kovalenko, V.I., Ryabchikov, I.D., and Antipin, V.S., 1988, Temperature dependence of the distribution coefficients for Sn, W, Pb, and Zn in magmatic systems: Geochemistry International, v. 25, no. 1, p. 1-10.

Kovalenko, V.I., Tsaryeva, G.M., Goreglyad, A.V., Yarmoluk, V.V., and Troitsky, V.A., 1995, The peralkaline-granite related Khaldzan-Buregtey rare metal (Zr, Nb, REE) deposit, western Mongolia: Economic Geology, v. 90, p. 530-547.

Kravchuk, I.F., Malinin, S.D., and Dernov-Pegarev, V.F., 1997, Tungsten behavior in a silicic fluid-magma system: Experimental Data: Geochemistry International, v. 35, p. 1083-1088.

Kravchuk, I.F., Malinin, S.D., and Varezhikina, N.S., 1990, Eu distribution between silicate melt and fluid at 800°C and 1.5 kbar: Geochemistry International, v. 27, no. 7, p. 82-91.

Lahti, S.I., 1987, Zoning in columbite-tantalite crystals from the granitic pegmatites of the Erajarve area, southern Finland: Geochimica et Cosmochimica Acta, v. 51, p. 509-517.

Lehmann, B., 1990, Metallogeny of tin: Lecture Notes in Earth Sciences, Springer-Verlag, Berlin, v. 32, 211 p.

Lindsey, D.A., 1977, Epithermal beryllium deposit in water laid tuffs, western Utah: Economic Geology, v. 72, p. 219-232.

Linnen, R.L., 1998, The solubility of Nb-Ta-Zr-Hf-W in granitic melts with Li and Li+F: Constraints for mineralization in rare-metal granites and pegmatites: Economic Geology, v. 93, p. 1013-1025.

Linnen, R.L., 2005, The effects of water on the solubility of accessory minerals in granitic melts: Lithos, v. 80, p. 267-280.

Linnen, R.L., and Keppler, H., 1997, Columbite solubility in granitic melts: Consequences for the enrichment and fractionation of Nb and Ta in the Earth's crust: Contributions to Mineralogy and Petrology, v. 128, p. 213-227.

Linnen, R.L., and Keppler, H., 2002, Melt composition control of Zr/Hf fractionation in magmatic processes: Geochimica et Cosmochimica Acta, v. 66, p. 3293-3301.

Linnen, R.L., Pichavant, M., and Holtz, F., 1996, The combined effects of f_{O_2} and melt composition on SnO_2 solubility and tin diffusivity in haplogranitic melts: Geochimica et Cosmochimica Acta, v. 60, p. 4965-4976.

Linnen, R.L., Pichavant, M., Holtz, F., and Burgess, S., 1995, The effect of f_{O_2} on the solubility, diffusion and speciation of tin in granitic melts at 850°C and 2 kbar: Geochimica et Cosmochimica Acta, v. 59, p. 1579-1588.

Linnen, R.L., and Williams-Jones, A.E., 1993, Mineralogical constraints on magmatic and hydrothermal Sn-W-Ta-Nb mineralization at the Nong Sua aplite-pegmatite deposit, Thailand: European Journal of Mineralogy, v. 5, p. 721-736.

Linnen, R.L., and Williams-Jones, A.E., 1994, The evolution of pegmatite-hosted tin-tungsten mineralization at Nong Sua, Thailand: Evidence from fluid inclusions and stable isotopes: Geochimica et Cosmochimica Acta, v. 58, p. 735-747.

London, D., 1986, Magmatic-hydrothermal transition in the Tanco rare-element pegmatite: Evidence from fluid inclusions and phase-equilibrium experiments: American Mineralogist, v. 71, p. 376-395.

London, D., 1987, Internal differentiation of rare-element pegmatites: Effects of boron, phosphorous, and fluorine: Geochimica et Cosomchimica Acta, v. 51, p. 403-420.

London, D., 1995, Geochemical features of peraluminous granites, pegmatites, and rhyolites as sources of lithophile metal

deposits: *in* Thompson, J.F.H., ed., Magmas, Fluids, and Ore Deposits, Mineralogical Association of Canada Short Course, v. 23, p. 175-198.

London, D., 2005, Geochemistry of alkalis and alkaline earths in ore-forming granites, pegmatites, and rhyolites: *in* Linnen, R.L., and Samson, I.M., eds., Rare-Element Geochemistry and Mineral Deposits, Geological Association of Canada Short Course Notes, v. 17, p. 17-43.

London, D., 2005b, Granitic pegmatites: An assessment of current concepts and directions for the future: Lithos, v. 80, p. 281-303.

London, D., Evensen, J.M., Fritz, E., Icenhower, J.P., Morgan, G.B. VI, and Wolf, M.B., 2001, Enrichment and accommodation of manganese in granite-pegmatite systems: 11th Annual Goldschmidt Conference Abstract 3369, Lunar Planetary Institute Contribution 1088, Lunar Planetary Institute, Houston (CD-ROM).

London, D., Hervig, R.L., and Morgan, G.B.VI., 1988, Melt-vapor solubilities and elemental partitioning in peraluminous granite-pegmatite systems: experimental results with Macusani glass at 200 MPa: Contributions to Mineralogy and Petrology, v. 99, p. 360-373.

London, D., Morgan, G.B.VI., Babb, H.A., and Loomis, J.L., 1993, Behaviour and effects of phosphorus in the system Na_2O-K_2O-Al_2O_3-SiO_2-P_2O_5-H_2O at 200 MPa (H_2O): Contributions to Mineralogy and Petrology, v. 113, p. 450-465.

London, D., Morgan, G.B.VI., and Hervig, R.L., 1989, Vapor-undersaturated experiments with Macusani glass + H_2O at 200 MPa, and the internal differentiation of granitic pegmatites: Contributions to Mineralogy and Petrology, v. 102, p. 1-17.

Manning, D.A.C., 1981, The effect of fluorine on liquidus phase relationships in the system Qz-Ab-Or with excess water at 1 kb: Contributions to Mineralogy and Petrology, v. 76, p. 206-215.

Manning, D.A.C., 1983, Chemical variations in garnets from aplites and pegmatites, peninsular Thailand: Mineralogical Magazine, v. 47, p. 353-358.

Manning, D.A.C., and Henderson, P., 1984, The behaviour of tungsten in granitic melt-vapour systems: Contributions to Mineralogy and Petrology, v. 86, p. 286-293.

Manning, D.A.C. and Hill, P.I., 1990, The petrogenetic and metallogenetic significance of topaz granite from the Southwest England orefield: Geological Society of America Special Paper 246, p. 51-69.

Marignac, C., and Cuney, M., 1999, Ore deposits of the French Massif Central: insight into the metallogenesis of the Variscan collision belt: Mineralium Deposita, v. 34, p. 472-504.

Marr, R.A., Baker, D.R., and Williams-Jones, A.E., 1998, Chemical controls on the solubility of Zr-bearing phases in simplified peralkaline melts and application to the Strange Lake intrusion, Quebec-Labrador: Canadian Mineralogist, v. 36, p. 1001-1008.

Martin, J.S., and Henderson, C.M.B., 1984, An experimental study on the effects of small amounts of lithium on the granite system: *in* Henderson, C.M.B., ed., Progress in Experimental Petrology, Environmental Research Council Publication Series D, v. 25, p. 30-35.

McDonough, W.F., and Sun, S.-s., 1995, The composition of the Earth: Chemical Geology, v. 120, p. 223-253.

Mitchell, R.H., 2005, Mineralogical and experimental constraints on the origin of niobium mineralization in carbonatites: *in* Linnen, R.L., and Samson, I.M., eds., Rare-Element Geochemistry and Mineral Deposits, Geological Association of Canada Short Course Notes, v. 17, p. 201-215.

Monier, G., Charoy, B., Cuney, M., and Ohnenstetter, D., 1987, Évolution spatiale et temporelle de la composition des micas du granite albitique à topaze-lépidolite de Beavoir: Géologie de la France, v. 1, no 2-3, p. 179-188.

Montel, J.-M., 1986, Experimental determination of the solubility of Ce-monazite in SiO_2-Al_2O_3-K_2O-Na_2O melts at 800°C, 2 kbar, under H_2O-saturated conditions: Geology, v. 14, p. 659-662.

Montel, J.-M., 1993, A model for monazite/melt equilibrium and application to the generation of granitic magmas: Chemical Geology, v. 110, p. 127-146.

Morgan, G. B. VI., and London, D., 1987, Alteration of amphibolitic wallrocks around the Tanco rare-element pegmatite, Bernic Lake, Manitoba: American Mineralogist, v. 27, p. 1097-1121.

Mungall, J.E., Dingwell, D.B., and Chaussidon, M., 1999, Chemical diffusivities of 18 trace elements in granitoid melts: Geochimica et Cosmochimica Acta, v. 63, p. 2599-2610.

Nekrasov, I.Y., Epel, and Sobolev, V.P., 1980, Partitioning of tin between melt and chloride fluid in the granite-SnO-SnO_2-fluid system: Doklady Earth Science Section, v. 252, p. 165-168.

Nielsen, R.L., and Beard, J.S., 2000, Magnetite-melt HFSE partitioning: Chemical Geology, v. 164, p. 21-34.

Ohnenstetter, D., and Piantone, P., 1992, Pyrochlore-group minerals in the Beauvoir peraluminous leucogranite, Massif-Central, France: Canadian Mineralogist, v. 30, p. 771-784.

Partington, G.A., 1990, Environment and structural controls on the intrusion of the giant rare metal Greenbushes pegmatite, Western Australia: Economic Geology, v. 85, p. 437-456.

Partington, G.A., McNaughton, N.J., and Williams, I.S., 1995, A review of the geology, mineralization, and geochronology of the Greenbushes pegmatite, Western Australia: Economic Geology, v. 90, p. 616-635.

Pichavant, M., Boher, M., Stenger, J.F., Aissa, M., and Charoy, B., 1987a, Relations de phase des granites de Beauvoir a 1 et 3 kbar en conditions de saturation en H_2O: Géologie de la France, no 2-3, p. 77-86.

Pichavant, M., Valencia Herrera, J., Boulmier, S., Briqueu, L., Joron, J.-L., Juteau, M., Marin, L., Michard, A., Sheppard, S.M.F., Treuil, M., and Vernet, M., 1987b, The Macusani glasses, SE Peru: evidence of chemical fractionation in peraluminous glasses: *in* Mysen, B.O., ed., Magmatic Processes: Physiochemical Principles. Geochemical Society Special Publication, v. 1, p. 359-373.

Pillet, D., Chenevoy, M., and Bélanger, M., 1992, Pétrologie du granite peralcalin du Lac Brisson, Labrador central, Nouveau Québec. 1. Mode de mise en palce et évolution chimique: Canadian Journal of Earth Sciences, v. 29, p. 353-372.

Pollard, P.J., 1989a, Geochemistry of granites associated with tantalum and niobium mineralization: *in* Möller, P., Černý, P., and, Saupé, F., eds., Lanthanides, Tantalum and Niobium, Springer Verlag, Berlin, p. 27-79.

Pollard, P.J., 1989b, Geologic characteristics and genetic problems associated with the development of granites-hosted deposits of tantalum and niobium: *in* Möller, P., Černý, P., and Saupé, F., eds, Lanthanides, Tantalum and Niobium, Springer Verlag, Berlin, p. 237-253.

Pollard, P.J., 1995, A special issue devoted to the geology of rare metal deposits. Geology of rare metal deposits: An introduction and overview: Economic Geology, v. 90, p. 489-494.

Pollard, P.J., Pichavant, M., and Charoy, B., 1987, Contrasting evolution of fluorine- and boron-rich tin systems: Mineralium Deposita, v. 22, p. 315-321.

Raimbault, L., 1998, Composition of complex lepidolite-type pegmatites and of constituent columbite-tantalite, Chèdeville, Massif Central, France: A subvolcanic equivalent of rare-metal granites: Canadian Mineralogist, v. 36, p. 563-583.

Raimbault, L., and Burnol, L., 1998, The Richemont rhyolite dyke (French Massif Central): A subvolcanic equivalent of rare-metal granites: Canadian Mineralogist, v. 36, p. 265-282.

Raimbault, L., Charoy, B., Cuney, M., and Pollard, P.J., 1991, Comparative geochemistry of Ta-bearing granites: *in* Pagel, M., and Leroy, J., eds., Source, Transport and Deposition of Metals. Rotterdam: Balkema, p. 793-796.

Raimbault, L., Cuney, M., Azencott, C., Duthou, J.L., and Joron, J.-L., 1995, Multistage magmatic genesis of a Ta-Sn-Li mineralized granite at Beauvoir, French Massif Central: A geochemical study: Economic Geology, v. 90, p. 548-576.

Rankin, A.H., 2005, Carbonatite-associated rare metal deposits: Composition and evolution of ore-forming fluids – the fluid inclusion evidence: *in* Linnen, R.L., and Samson, I.M., eds., Rare-Element Geochemistry and Mineral Deposits, Geological Association of Canada Short Course Notes, v. 17, p. 299-314.

Rapp, R.P., Ryerson, F.J., and Miller, C.F., 1987, Experimental evidence bearing on the stability of monazite during crustal anatexis: Geophysical Research Letters, v. 14, p. 307-310.

Rapp, R.P., and Watson, E.B., 1986, Monazite solubility and dissolution kinetics: implications for the thorium and light rare earth chemistry of felsic magmas: Contributions to Mineralogy and Petrology, v. 94, p. 304-316.

Reed, M.J., Candela, P.A., and Piccoli, P., 2000, The distribution of rare earth elements between monzogranitic melt and the aqueous volatile phase in experimental investigations at 800°C and 200 MPa: Contributions to Mineralogy and Petrology, v. 140, p. 251-262.

Renno, A., 1997, Zur Petrogenese der abite granite von Abu Dabbab and Nuweibi, Central Eastern Desert, Ägypten: unpub. PhD thesis, Berlin Technical University, 138 p.

Reyf, F.G., Seltmann, R., and Zaraisky, G.P., 2000, The role of magmatic processes in the formation of banded Li,F-enriched granites from the Orlovka tantalum deposit, Transbaikalia, Russia: microthermometric evidence: Canadian Mineralogist, v. 38, p. 915-936.

Salvi, S., and Williams-Jones, A.E., 2005, Alkaline granite-syenite hosted deposits: *in* Linnen, R.L., and Samson, I.M., eds., Rare-Element Geochemistry and Mineral Deposits, Geological Association of Canada Short Course Notes, v. 17, p. 315-341.

Samson, I.M., and Wood, S.A., 2005, The rare-earth elements: Behavior in hydrothermal fluids and concentration in hydrothermal mineral deposits, exclusive of alkaline settings: *in* Linnen, R.L., and Samson, I.M., eds., Rare-Element Geochemistry and Mineral Deposits, Geological Association of Canada Short Course Notes, v. 17, p. 269-297.

Schäfer, B., Frischknecht, R., Gunther, D., and Dingwell, D.B., 1999, Determination of trace-element partitioning between fluid and melt using LA-ICP-MS analysis of synthetic fluid inclusions in glass: European Journal of Mineralogy, v. 11, p. 415-426.

Schmitt, A.K., Emmermann, R., Trumbull, R.B., Bühn, B., and Henjes-Kunst, F., 2000, Petrogenesis and $^{40}Ar/^{39}Ar$ geochronology of the Brandberg Complex, Namibia: Evidence for a major mantle contribution in metaluminous and peralkaline granites: Journal of Petrology, v. 41, p. 1207-1239.

Selway, J.B.,Černý, P., and Hawthorne, F.C., 2000, The Tanco pegmatite at Bernic Lake, Manitoba. XIV. Internal tourmaline: Canadian Mineralogist, v. 38, p. 877-891.

Sirbescu, M.-L.C., and Nabelek, P.I., 2003, Crustal melts below 400°C: Geology, v. 31, p. 685-688.

Sowerby, J., and Keppler, H., 2002, The effect of fluorine, boron and excess sodium on the critical curve in the albite-H_2O system: Contributions to Mineralogy and Petrology, v. 143, p. 32-37.

Štemprok, M., 1990, Solubility of tin, tungsten and molybdenum oxides in felsic magmas: Mineralium Deposita, v. 25, p. 205-212.

Stewart, D.B., 1978, Petrogenesis of lithium-rich pegmatites: American Mineralogist, v. 63, p. 970-980.

Stimac, J., and Hickmot, D., 1994, Trace-element partition coefficients for ilmenite, orthopyroxene and pyrrhotite in rhyolite determined by micro-PIXE analysis: Chemical Geology, v. 117, p. 313-330.

Stussi, J.-M., and Cuney, M., 1993, Modèles d'évolution géochimique de granitoïdes peralumineux. L'exemple du complexe plutonique varisque du Millevaches (Massif central français): Bull. Soc. Géol. France, v. 164, p. 585-596.

Sun, S.-S., and McDonough, W.F., 1989, Chemical and isotopic systematics of oceanic basalts: implications for mantle composition and processes: *in* Saunders, A.D., and Norry, M.J., eds., Magmatism in the Ocean Basins, Geological Society of London Special Publication, v. 42, p. 313-345.

Sweetapple, M.T., and Collins, P.L.F., 2002, Genetic framework for the classification and distribution of Archean rare metal pegmatites in the North Pilbara Craton, Western Australia: Economic Geology, v. 97, p. 873-895.

Syritso, L.F., and Chernick, L.N., 1967, Evolution in accessory mineral paragenesis during metasomatic alteration of granites in eastern Transbaikalia massifs: International Geology Review, v. 9, p. 814-827.

Syritso, L.F., Tabuns, E.V., Volkova, E.V., Badanina, E.V., and Vysotskii, Y.A., 2001. Model for the genesis of Li-F granites in the Orlovka massif, Eastern Transbaikalia: Petrology, v. 9, p. 268-289.

Taylor, J.R.P., 1988, Experimental studies on tin in magmatic-hydrothermal systems: unpublished Ph.D. thesis, Monash University, Melbourne, Australia, 223 p.

Taylor, J.R., and Wall, V.J., 1992, The behaviour of tin in granitoid magmas: Economic Geology, v. 87, p. 403-420.

Taylor, R.P., 1992, Petrological and geochemical characteristics of the Pleasant Ridge zinnwaldite-topaz granite, Southern New Brunswick, and comparison with other topaz-bearing felsic rocks: Canadian Mineralogist, v. 30, p. 895-921.

Taylor, S.R., and McLennan, S.M., 1995, The geochemical evolution of the continental crust: Reviews of Geophysics, v. 33, p. 241-265.

Thomas, A.V., Bray, C.J., and Spooner, E.T.C., 1988, A discussion of the Jahns-Burnham proposal for the formation of zoned granitic pegmatites using solid-liquid-vapour inclusions from the Tanco pegmatite, S.E. Manitoba, Canada: Transactions of the Royal Society of Edinburgh: Earth Science, v. 79, p. 299-315.

Thomas, A.V., Pasteris, J.D., Bray, C.J., and Spooner, E.T.C., 1990, H_2O-CH_4-NaCl-CO_2 inclusions from the footwall contact of the Tanco granitic pegmatite: Estimates of internal pressure and composition from microthermometry, laser Raman spectroscopy, and gas chromatography: Geochimica et Cosmochimica Acta, v. 54, p. 559-573.

Thomas, R., Förster, H.F., and Heinrich, W., 2003, The behaviour of boron in a peraluminous granite-pegmatite system and associated hydrothermal solutions: a melt and fluid inclusion study):

Contributions to Mineralogy and Petrology, v. 144, p. 457-472.

Thomas, R., Rhede, D., and Trumbull, R.B., 1996, Microthermometry of volatile-rich silicate melt inclusions in granitic rocks: Z. Geol. Wiss., v. 24, p. 507-528.

Thomas, R., and Webster, J.D., 2000, Strong tin enrichment in a pegmatite-forming melt: Mineralium Deposita, v. 35, p. 570-582.

Thomas R., Webster, J.D., and Heinrich, W., 2000, Melt inclusions in pegmatite quartz: complete miscibility between silicate melts and hydrous fluids at low pressure: Contributions to Mineralogy and Petrology, v. 139, p. 394-401.

Tindle, A.G., and Breaks, F.W., 2000, Columbite-tantalite mineral chemistry from rare-element granitic pegmatites: Separation Lake area, N.W. Ontario, Canada: Contributions to Mineralogy and Petrology, v. 70, p. 165-198.

Tsareva, G.M., Naumov, V.B., Kovalenko, V.I., Tsepin, A.I., and Andreyeva, I.A., 1995, Magmatic cassiterite, wolframite, columbite, and tungstoixiolite in Volynia chamber pegmatites: Data from inclusions in topaz: Doklady Earth Science, v. 331, p. 175-178.

Turpin, L., Cuney, M., Friedrich, M., Bouchez, J.-L., and Aubertin, M., 1990, Meta-igneous origin of peraluminous granites in NW French Massif Central: implications for crustal history reconstructions: Contributions to Mineralogy and Petrology, v. 104, p. 163-172.

Veksler, I.V., 2005, Element enrichment and fractionation by magmatic aqueous fluids: Experimental constraints on fluid-melt immiscibility and element partitioning: *in* Linnen, R.L., and Samson, I.M., eds., Rare-Element Geochemistry and Mineral Deposits, Geological Association of Canada Short Course Notes, v. 17, p. 69-85.

Veksler, I., Thomas, R., and Schmidt, C., 2002, Experimental evidence of three coexisting immiscible fluids in synthetic granitic pegmatite: American Mineralogist, v. 87, p. 775-779.

Watson, E.B., 1979, Zircon saturation in felsic liquids: Experimental results and applications to trace element geochemistry: Contributions to Mineralogy and Petrology, v. 70, p. 407-419.

Watson, E.B., and Harrison, T.M., 1983, Zircon saturation revisited: temperature and composition effects in a variety of crustal magma types: Earth and Planetary Science Letters, v. 64, p. 295-304.

Webster, J.D., Holloway, J.R., and Hervig, R.L., 1987, Phase equilibria of a Be, U and F-enriched vitrophyre from Spor Mountain, Utah: Geochimica et Cosmochimica Acta, v. 51, p. 389-402.

Webster, J.D., Holloway, J.R., and Hervig, R.L., 1989, Partitioning of lithophile trace elements between H_2O and H_2O+CO_2 fluids and topaz rhyolite melt: Economic Geology, v. 84, p. 116-134.

Webster, J.D., Thomas, R., Rhede, D., Forster, H.-J., and Seltmann, R., 1997, Melt inclusions in quartz from an evolved peraluminous pegmatite: Geochemical evidence for strong tin enrichment in fluorine-rich and phosphorous-rich residual liquids: Geochimica et Cosmochimica Acta, v. 61, p. 2589-2604.

Wedepohl, K.H., 1995, The composition of the continental crust: Geochimica et Cosmochimica Acta, v. 59, p. 1217-1239.

White, A.J.R., and Chappell, B.W., 1977, Ultrametamorphism and granite genesis: Tectonophysics, v. 43, p. 7-22.

Wilson, G. A., and Eugster, H. P., 1990, Cassiterite solubility and tin speciation in supercritical chloride solutions: *in* Spencer, R.J., and Chou, I.M., eds., Geochemical Society Special Publication, v. 2, p. 179-195.

Wolf, M.B., and London, D., 1993, Preliminary results of HFS and RE element solubility experiments in 'granites' as a function of B and P: EOS, v. 74, p. 343.

Wolf, M.B., and London, D., 1995, Incongruent dissolution of REE- and Sr-rich apatite in peraluminous granitic liquids: Differential apatite, monazite, and xeontime solubilities during anatexis: American Mineralogist, v. 80, p. 765-775.

Wolf, M.B., London, D., and Morgan, G.B. VI., 1994, Effects of boron on the solubility of cassiterite and tantalite in granitic liquids: Geological Society of America Abstracts with Program, v. 26, p. A-450.

Wood, S.A., 2005, The aqueous geochemistry of zirconium, hafnium, niobium and tantalum: *in* Linnen, R.L., and Samson, I.M., eds., Rare-Element Geochemistry and Mineral Deposits, Geological Association of Canada Short Course Notes, v. 17, p. 217-268.

Wood, S.A., and Samson, I.M., 2000, The hydrothermal geochemistry of tungsten in granitoid environments: I. Relative solubilities of ferberite and scheelite as a function of T, P, pH and m_{NaCl}: Economic Geology, v. 95, p. 143-182.

Yin, L., Pollard, P.J., Shouxi, H., and Taylor R.G., 1995, Geological and geochemical characteristics of the Yichun Ta-Nb-Li deposit, Jiangxi Province, south China: Economic Geology, v. 90, p. 577-585.

Zhalashkova, N.Y., and Sitnin, A.A., 1967, Features of the distribution of rare elements in tatalum-bearing apogranites and biotite granites: Geochemistry International, v 4, p. 1013-1025.

Zhu, J-C., Li, R-K, Li, F-C, Xiong, X-L., Zhou, F-Y., and Huang, X-L., 2001, Topaz-albite granites and rare metal mineralization in the Limu district, Guangxi Province, southeast China: Mineralium Deposita, v. 36, p. 393-405.

Keywords: granite, pegmatite, peralkaline, peraluminous, Ta, Nb, W, Sn, Zr, Hf.